Thesis

CHONDROCYTE APOPTOSIS FOLLOWING GROWTH PLATE STIMULATION AFTER FRACTURE

Submitted by

Sonja Gaber

Mat. Nr. 0211602

In order to attain the academic degree

Doctor medicinae universae

(Dr. med. univ.)

at the

Medical University of Graz

Clinic for Paediatric Surgery

Supervised by

Priv. Doz. Dr. Annelie-Martina Weinberg

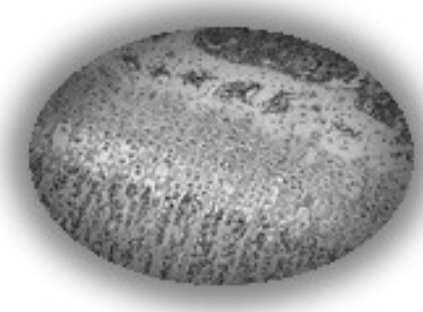

Graz, September 2008

Eidesstattliche Erklärung

Ich erkläre ehrenwörtlich, dass ich die vorliegende Arbeit selbstständig und ohne fremde Hilfe verfasst habe, andere als die angegebenen Quellen nicht verwendet habe und die den benutzten Quellen wörtlich oder inhaltlich entnommenen Stellen als solche kenntlich gemacht habe.

Graz, am 20. September 2008 *Gaber Sonja*

Acknowledgements

First of all, I am deeply indebted to my supervisor, Priv.-Doz. Dr. Annelie-Martina Weinberg, for her guidance and advice, for fruitful discussions and comments, and for introducing me to scientific research and providing me with the great opportunity to work within her research group.

I would like to thank all members of this research group for their assistance and co-operation, especially Mag. Peter Blümel for his support in laboratory works and for his perseverance in manual cell counting, Dr. Eva Elisa Fischerauer for her help with routine problems and her willingness to proofread this thesis, and Dr. Gregor Janezic for introducing me to basic laboratory works.
I am also grateful for the help of Mag. Andrea Groselj-Strele in statistical analyses, Prof. Dr. Eleonore Fröhlich for answering all my questions concerning immunohistochemical methods, and Dr. Emir Haxhija for his advice on TUNEL staining.

Furthermore, I must express special thanks to Alice Clare Grigg for proofreading my thesis, to Alexander Müller who assisted me in drawing the figures used in this work, and to my parents for their love, encouragement and understanding throughout my studies.

This work was supported by a research grant from the Medical University of Graz.

Abstract

Introduction: Post-traumatic overgrowth of long bones is a common clinical phenomenon in paediatric traumatology and is to be expected when faced with a fractured growing bone. Accelerated bone growth after fracture is the result of an enhanced stimulation of the nearby growth plate. However, up till now the exact post-fractural reactions of the growth plate are poorly understood. This study aims to determine the impact of fracture on chondrocyte apoptosis in the growth plate.

Methods: Fifty-six male Sprague-Dawley rats weighing between 100 and 120 g were randomly distributed into two main groups, the experimental and the control group, and these were further divided into 4 subgroups with 7 rats in each. Animals in the experimental group sustained a middiaphyseal closed fracture of the left tibia using a standardised guillotine. Euthanasia was performed 3, 10, 14 and 29 days after fracture. The control rodents were sacrificed at the same time. The left and right tibiae were harvested, fixed in formaldehyde, decalcified and embedded in paraffin. Finally, apoptotic chondrocytes of the proximal tibial growth plate were detected by the use of TUNEL staining, which labels DNA fragmentations, the hallmark of apoptosis. Apoptotic cell bodies were manually counted by means of light microscopy and the apoptosis percentage of physeal chondrocytes was statistically compared between the fractured bone, the intact contra-lateral bone and the control bone.

Results: The physeal apoptosis rate of the fractured bone was significantly higher than that of the intact contra-lateral bone (valid for all evaluated days) and that of the control bone (valid from day 10 onwards). Contra-lateral intact tibiae never showed physeal apoptosis rates which were significantly higher than that of the control tibiae.

Discussion: This study provides evidence that a middiaphyseal fracture influences the nearby growth plate by stimulating chondrocyte programmed cell death, which is associated with cartilage resorption and bone replacement. The lack of a significant difference between the intact contra-lateral bone and the intact control bone suggests that there is a local effect of the fracture which contributes to the higher apoptosis rate of the adjacent physis.

Zusammenfassung

Einleitung: Stimulative Wachstumsphänomene sind obligatorisch nach sämtlichen im Wachstumsalter auftretenden Frakturen langer Röhrenknochen zu erwarten. Ursächlich wird eine durch die Fraktur ausgelöste gesteigerte Funktion angrenzender Epiphysenfugen beschrieben. Der genaue Mechanismus dieser Aktivitätssteigerung ist jedoch unbekannt. Ziel dieser experimentellen Studie war es, die posttraumatische Reaktion der Wachstumsfuge auf zellulärer Ebene zu bestimmen und frakturierte Knochen mit Kontrollknochen bezüglich der Rate an apoptotischen Chondrozyten in der Epiphysenfuge zu vergleichen.

Methodik: 56 männliche, 100 bis 120 g schwere Sprague-Dawley-Ratten wurden einer Experimental- und einer Kontrollgruppe zugeordnet, wovon den Experimentaltieren mittels einer Guillotine eine geschlossene Schaftfraktur der linken Tibia zugefügt wurde. Je nach Zugehörigkeit zu Subgruppen erfolgte die Tötung der Ratten 3, 10, 14 oder 29 Tage nach dem Setzen der Fraktur, auch die Kontrolltiere wurden zu den gleichen Zeitpunkten getötet. Die TUNEL-Färbung, welche die Darstellung Apoptose-spezifischer DNA Fragmente ermöglicht, wurde zur Bestimmung der chondrozytären Apoptoserate der proximalen tibialen Wachstumsfuge durchgeführt. Anschließend wurde der Prozentsatz apoptotischer Knorpelzellen für den frakturierten Knochen, den kontralateralen intakten Knochen sowie für die linke Kontrolltibia mittels Lichtmikroskopie bestimmt.

Ergebnisse: Der frakturierte Knochen wies, verglichen mit dem kontralateralen ungebrochenen Bein, an allen posttraumatischen Tagen und, verglichen mit dem Kontrollknochen, an den Tagen 10, 14 und 29 eine signifikant höhere Apoptoserate der Zellen der Epiphysenfuge auf. Das intakte rechte Bein des Experimentaltieres hingegen zeugte von keiner relevanten Erhöhung des programmierten Zelltodes gegenüber dem Kontrolltier.

Diskussion: Die Fraktur wirkt sich auf die angrenzende Epiphysenfuge mit einer Zunahme des programmierten Zelltodes, welcher für die Knorpelresorption und Knochenneubildung unerlässlich ist, aus. Dabei dürfte ein lokal wirkender Effekt der Fraktur auf die Wachstumsfuge eine größere Rolle spielen als systemische Einflussgrößen, welche auch ein Ansteigen der Apoptoserate im intakten Knochen des Experimentaltieres gegenüber dem Kontrolltier zur Folge gehabt hätten.

Table of Contents

1. Introduction 1

1.1. Aim of the Study 3

2. Background 5

2.1. Anatomical, Physiological and Histological Bone Aspects 5

2.1.1. Bone Types 6

2.1.2. Macrostructure of a Tubular Bone 7

2.1.3. Microstructure of a Tubular Bone 9

2.1.4. Extracellular Matrix of Bone Tissue 10

2.1.5. Cell Types of Bone Tissue 12

2.2. Long Bone Development and Growth 18

2.2.1. Cartilage Cells and Matrix 19

2.2.2. Endochondral Ossification of Long Bones 20

2.2.3. The Growth Plate 22

2.2.4. Vascular Supply of the Physis 25

2.2.5. Growth of Bone Diameter 26

2.2.6. Regulation of Longitudinal Growth at the Growth Plate 26

2.3. Fracture Healing 29

2.3.1. Fracture Repair Sequence 30

2.3.2. Molecular Control of Fracture Healing 32

2.4. Apoptosis 35

2.4.1. Tools for the Study of Apoptosis 40

3. Materials and Methods 42

3.1. Materials 42

3.2. Animal Experiments and Protocols 45

3.2.1. The Fracture 47

3.2.2. Euthanasia 47

3.3. The Treatment of the Bones 48

3.4. TUNEL Assay 49
3.4.1. Tissue Preparation 50
3.4.2. Proteinase K 51
3.4.3. Hydrogen Peroxide 51
3.4.4. TUNEL Reaction 51
3.4.5. Signal Conversion 52
3.4.6. Control Sections 53
3.5. Digital Slide Images 53
3.6. Quantification of Apoptotic Cells 53
3.6.1. Partition of the Growth Plate into Different Regions and Zones 54
3.7. Statistical Analyses 56
4. Results 57
4.1. Fractured Bone versus Contra-lateral Bone 57
4.2. Fractured Bone versus Control Bone 58
4.3. Contra-lateral Bone versus Control Bone 61
4.4. Columnar Zone versus Hypertrophic Zone 61
5. Discussion 65
5.1. The Rat Model 65
5.2. Fate of Hypertrophic Chondrocytes 66
5.3. Apoptosis Detection with TUNEL – A Controversial Subject 68
5.4. Increased Growth Plate Apoptosis after Fracture 70
5.5. Age-dependency of Physeal Chondrocyte Apoptosis 71
5.6. Columnar versus Hypertrophic Chondrocytes 71
References 73

List of Figures

Figure 1: Boy with leg length discrepancy as a result of overgrowth after femoral fracture 3

Figure 2: Components of a typical long bone during growth 7

Figure 3: Components of bone tissue 11

Figure 4: The development of tissue-specific cells from a pluripotent mesenchymal progenitor cell 13

Figure 5: Bone resorption by the osteoclast 16

Figure 6: The regulation of osteoclast differentiation and activation by osteoblasts. 18

Figure 7: The stages of endochondral ossification in a long bone 22

Figure 8: A section of the proximal growth plate of a rat tibia 24

Figure 9: Major extrinsic and intrinsic molecules controlling the growth plate 27

Figure 10: Schematic model of feedback loops and biological activities of Ihh, PTHrP, FGFs and BMPs in the growth plate 29

Figure 11: Different stages of secondary fracture healing 32

Figure 12: Schematic summary of the temporal expression patterns of TGF-β superfamily members during animal fracture healing 34

Figure 13: Schematic representation of apoptotic signalling from the plasma membrane, mitochondrium, nucleus and endoplasmic reticulum 40

Figure 14: Sprague-Dawley rats in their litters 46

Figure 15: Unfractured right tibia of a rat weighing 165 g 48

Figure 16: Tibia with marked growth plate 48

Figure 17: Arrangement of tissue sections on microscope slides 50

Figure 18: TUNEL-positive chondrocytes..... 54

Figure 19: Tibial growth plate - division into 3 regions 54

Figure 20: Tibial growth plate - division into 2 zones 55

Figure 21: The apoptosis percentages of the fractured left and unfractured right tibiae of the experimental group are shown in graph. 58

Figure 22: The apoptosis rates (in %) of the fractured left tibia of the experimental group and of the left tibia of the control group are shown in graph..... 59

Figure 23: The apoptosis rates (in %) of the fractured left tibia of the experimental group and of the left tibia of the control group were analysed separately for the columnar zone and the hypertrophic zone of the growth plate 60

Figure 24: Physeal apoptosis rates (in %) of the right intact tibia of the experimental group compared to the left intact tibia of the control group 62

Figure 25: Light microscopy of several TUNEL-stained growth plate sections 63

Figure 26: TUNEL method control sections 64

List of Tables

Table 1: Animals and pharmaceuticals 42

Table 2: Chemicals 43

Table 3: Laboratory instruments and consumables 44

Table 4: Laboratory equipment 44

Table 5: Animal allocation into groups 46

Table 6: Summary of the physeal apoptosis rates (in %) of the left and right tibiae of the experimental group 57

Table 7: Summary of the physeal apoptosis rates (in %) of the left tibia of the experimental group and of the left tibia of the control group 61

Abbreviations

AA	arachidonic acid
AIF	apoptosis inducing factor
Apaf-1	apoptotic protease activating factor-1
ATF6	activating transcription factor 6
Bcl-2	B cell lymphoma protein 2
Bcl-xL	Bcl extra long
BH3	bcl-2 homology domain
Bid	BH3 domain-only death agonist
BMPs	bone morphogenetic proteins
Ca^{2+}	calcium
CAD	caspases-activated DNase
CD	cluster of differentiation
CSF-1	colony stimulation factor-1
DAB	diaminobenzidine
dADP	deoxyadenosine diphosphate
dATP	deoxyadenosine triphosphate
DNA	deoxyribonucleic acid
DR	death receptor
dUTP	deoxyuridine triphosphate
ELISA	enzyme-linked immunosorbent assay
ER	endoplasmic reticulum
FADD	Fas-associated death domain protein
FGF	fibroblast growth factor
GDF	growth and differentiation factor
Gla-proteins	gamma-carboxy glutamic acid-containing proteins
Gtt	Guttae (Latin for drops)
HCl	hydrogen chloride
HtrA2/Omi	high temperature requirement A2 protein
IAPs	inhibitor of apoptosis proteins
IGF-1	insulin-like growth factor 1
Ihh	Indian hedgehog

IKK	IκB kinase
IL	interleukin
Ire1	type 1 endoplasmic reticulum transmembrane protein kinase
IκB	inhibitor of κB
M-CSF	macrophage-colony stimulating factor
MMPs	matrix metallproteinases
NF-κB	nuclear factor κB
OH	hydroxide
OPG	osteoprotegerin
PARP	polyadenosine ribose polymerase
PBS	phosphate buffered saline
PGE_2	prostaglandin E2
PI-3 kinase	phosphoinositide 3 kinase
PIP2	phospatidylinositol 4,5-disphosphate
PIP3	phospatidylinositol 3,4,5-trisphosphate
PKB	protein kinase B
PLA2	phospholipase A2
POD	horse-radish peroxidase
Ptch1	Patched-1
PTH	parathyroid hormone
PTHrP	parathyroid hormone-related peptide
RANK	receptor activator nuclear factor κB
RANKL	receptor activator nuclear factor κB ligand
RIP-1	receptor interacting protein 1
Smac	second mitochondria-derived activator of caspases
Smo	smoothened
tBid	truncated BH3 domain-only death agonist
TdT	terminal deoxynucleotidyl transferase
TGF-β	transforming growth factor-β
TNF	tumor necrosis factor
TNF-α	tumor necrosis factor α
TRADD	TNF receptor-associated death domain protein
TRAF-2	TNF receptor-associated factor 2
TRAIL	tumor necrosis factor-related apoptosis-inducing ligand

TUNEL	terminal deoxynucleotidyl transferase (TdT)-mediated dUTP nick end labelling
VEGF	vascular endothelial growth factor
VEGFR	vascular endothelial growth factor receptor

1. INTRODUCTION

The growing skeleton shows exceptional advantages in the healing of bone fractures, such as the short length of time needed for union, the rare appearance of delayed union or non-union, and the capacity for spontaneous remodelling of post-traumatic bone deformities including sideway shift, angulation and even rotational deformities. With regard to these advantages, paediatric fractures differ from adult fractures and therefore require distinct and specifically adapted therapeutical strategies. [1] The mechanism of spontaneous correction can be subsumed within the term “growth phenomenon” [1]. The remodelling ability of a child’s bone makes reduction accuracy less important than with the adult bone; conservative treatment of paediatric fractures is common practice. Unnecessary reductions, anaesthesia and post-traumatic deformities can be avoided. [2,3]

Moreover, bone fractures of the growing skeleton are unique in their potential to develop growth disturbances, another type of growth phenomenon. Stimulating growth disturbances, referring to the overgrowth of bones, must be distinguished form inhibited growth disturbances, during which growth arrest or growth inhibition occurs. [4] Overgrowth represents a clinical complication of fractured growing bones and can only occur if the corresponding epiphyseal plates of the fractured long bone have not yet closed. Stimulating growth phenomena are associated with an elevated function of the growth plate, which can be affected either wholly or partially. The former results in limb length discrepancy; the latter leads to angular and joint deformities and presents an established risk factor in the development of early arthrosis. [5] Concerning the upper extremities, differences in length do not affect functionality and are therefore clinically insignificant, whereas leg length discrepancy can lead to gait abnormalities, pelvic obliquity with subsequent lumbar scoliosis, functional disturbances of hip, knee and ankle joints and can also cause psychological problems. [6]

Post-traumatic overgrowth should be obligatorily expected in every fractured growing bone and is the result of an enhanced stimulation of the nearby growth plate. In the majority of cases the whole of the physis is affected, whereas a partial

stimulation of the growth plate has been rarely observed, most likely to occur at the distal humerus and the proximal tibia after metaphyseal bending fractures. [4,5] Overgrowth occurring after femoral shaft fracture has been well documented in a range of retrospective trials. [7-11]

The occurrence of stimulating growth disorders seems to be heavily dependent on the age of the child concerned and less so on the location of the fracture. During growth years, the incidence and the extent of post-traumatic overgrowth is at a peak, whereas fracture that takes place during the premature age (the time of physeal resting immediately before physeal closure) initially leads to an increased growth but then to a premature closure of the physis, resulting in a slight shortening of the bone. This usually means that patients under the age of 10 have to deal with stimulated growth, while children older than 10 are more likely to suffer from bone shortening. [1,4,5]

Laer and colleagues showed the presence of a post-traumatic leg length difference in 70% of cases after femoral shaft fractures and in 40% of cases after tibial and fibular fractures. In the control group, an idiopathic difference in limb length was found in 25% of cases. Furthermore, they defined average overgrowth as 10 mm following a femoral fracture and as 7 mm following a fracture of the lower leg. [12] It is speculated that the responsible factors for physeal stimulation may be, on the one hand, an increased blood flow to the adjacent growth plates and, on the other hand, the influence of hormones and growth factors. [1,5] In a follow-up study of 149 paediatric fractures of the femoral shaft, Laer and co-workers highlighted the significant influence of multiple reduction manoeuvres and residual axial deviations on the incidence and extent of post-traumatic overgrowth. Furthermore, he demonstrated that therapeutic shortening of the fractured bone at the time of initial reduction cannot prevent future lengthening; this therapeutic strategy can even enhance overgrowth due to the increased stimulation of repair mechanisms at the growth plate. [13] Today it is generally accepted that repeated and late reductions after paediatric fractures should be avoided. In contrast to fractures of the upper extremities, spontaneous correction should not be obligatorily integrated in the treatment of fractures of the lower extremities as it provokes increased remodelling, resulting in the activation of the adjacent growth plates. [5] Instead, a definite and early stabilisation of the fracture with anatomical

alignment and without shortening should be used in order to prevent stimulating growth disorders. [1,5,12] According to Hasler and colleagues, in metal plate osteosyntheses, the removal of metal acts as an additional stimulus to the growth plate. [5]

However, up till now the underlying molecular mechanisms that stimulate growth in the growth plate after fracture have not been fully clarified.

Figure 1: Boy with leg length discrepancy as a result of overgrowth after femoral fracture. (Photographs were kindly provided by the University Clinic of Paediatric Surgery, Graz.)

1.1. Aim of the Study

Post-traumatic growth disturbances are a common clinical phenomenon in paediatric traumatology. However, to date, there is less information on the molecular response of the growth plate to long bone fracture of the growing skeleton, which may lead to unique post-traumatic overgrowth in children. In order to gain more information about the post-fractural reactions of physeal cells, this

study aims to determine the impact of fracture on cellular apoptosis in the growth plate of rats. Apoptosis is one indication of physeal cell turnover which is hypothesised to be stimulated by fracture. This work will benefit the understanding of the effect of post-fractural reactions on the growth plate.

Animals in the experimental group sustained a middiaphyseal closed fracture of the left tibia and were extensively compared to control animals. Apoptosis of physeal chondrocytes was determined by the use of TUNEL staining. The three focal questions which the study aimed to evaluate were specified prior to the experiments:

- To what extent do the physeal apoptosis rates of the fractured left tibia and of the intact contra-lateral right tibia differ in the experimental group?
- To what extent are the apoptosis rates of the growth plates of the fractured left tibia of the experimental group and of the unfractured left tibia of the control group different?
- What is the difference between the physeal apoptosis rates of both intact bones (the right unfractured tibia of the experimental animal and the left unfractured tibia of the control animal)?

All investigations were carried out on days 3, 10, 14 and 29 post-fracture.

2. BACKGROUND

2.1. Anatomical, Physiological and Histological Bone Aspects

The skeleton is an extremely specialised form of connective tissue of which the two main types are bone and cartilage. [14] Skeletal bones have different functions, such as the provision of a rigid framework for the protection of vital organs and for the attachment of muscles, tendons and ligaments. Bones allow movement by means of articulations, serve as levers that turn muscle contraction into useful movements and function as struts to counter the force of gravidity affecting the body. The formation of blood cells from haematopoietic tissue in the red bone marrow mostly takes place in the short, flat and irregular bones. Moreover, bones are essential for calcium and phosphorus homeostasis by acting as reservoirs for the above mentioned electrolytes. [15]

The adult skeleton contains between 1 and 2 kg of calcium and between 0.5 and 0.75 kg of phosphorus which means that 99% of the total level of calcium and 88% of the total level of phosphorus are stored in the bones. [15] The regulation of the mobilisation and release of skeletal calcium and phosphate and the promotion of mineralisation of bones, is under hormone and cytokine control. 1,25-dihydroxycholecalciferol (synonym: calcitriol), parathyroid hormone (PTH) and calcitonin act as the main regulators of calcium metabolism. In addition, glucocorticoids, growth hormone, oestrogen, thyroid hormones, insulin and insulin-like growth factor 1 (IGF-1) are also involved in calcium regulatory processes. [16]

Bone can be regarded as a dynamic tissue with a high rate of metabolic activity. [15] New bone is constantly being formed while old bone is being resorbed. In adults, approximately 10% of bone tissue is replaced each year, resulting in a complete renewal every 10 years. [17] This kind of remodelling allows osseous tissue to respond to the mechanical stresses and strains to which they are constantly exposed. In order to perpetuate this process of permanent structural alteration, bone tissue is well vascularised with an overall blood flow of 200 to 400 ml/min in adult humans. [18]

During foetal life, the human skeleton mainly consists of cartilage tissue that is gradually replaced by bone. In adults, cartilage remains in the larynx, epiglottis, trachea, bronchi, nose, external ears and intervertebral discs. Cartilage can also still be found on the articular surfaces of long bones, as it is an important component of synovial joints. The epiphyseal plate, which is responsible for the longitudinal growth of tubular bones during childhood, is made up of hyaline cartilage as long as the physis is not closed and replaced by osteal tissue. [19] In contrast to bones, cartilaginous tissues possess an extremely low metabolic rate with an extracellular matrix that is neither vascularised nor innervated. [14] Chondrocytes, the main cell type of cartilage, are used to living in a low oxygen tension environment [14] and receive their nutrition and oxygen predominantly by diffusion.

2.1.1. Bone Types

Generally, bones can be divided into long, short, flat, irregular, pneumatic, sesamoid and accessory bones. [20] Examples of long bones are the tubular (or pipe) bones of the limbs (Figure 2). They consist of a central shaft called the diaphysis, and an epiphysis at each end. The metaphysis is located between these two parts and is defined as the wider section located at both ends of the diaphysis. [21] During growth the diaphysis and each corresponding epiphysis are separated by the growth plate (the epiphyseal plate or the physis) which consists of hyaline cartilage and is responsible for the longitudinal growth of bones. When growth is completed, the physis becomes fully calcified and remains as the epiphyseal line. [15]

The carpal and tarsal bones are classified as short bones. In contrast to long bones, they are cube-shaped and mainly composed of cancellous bone enveloped in a thin layer of compact bone. Flat bones are those of a thin shape with two parallel layers of compact bone sandwiching one layer of spongy bone. The scapula, ilium, sternum, ribs and bones of calvaria are examples of flat bones. Irregular bones, characterised by an irregular and inconsistent shape, include the vertebrae and bones of the skull base. [20,22]

In adults, only short, flat and irregular bones contain red marrow with haematopoietic tissue content; they are therefore cardinal locations for blood cell production. [15]

Some bones of the facial skeleton and paranasal sinuses contain air-filled cavities and are therefore given the nomenclature of pneumatic or pneumaticed bones. Sesamoid bones, such as the patella, are embedded in tendons; accessory bones are anomalous, supernumerary bones resulting from the lack of fusion of an ossification centre. They appear in the hand, foot and calvaria and involve the risk of being wrongly diagnosed as a displaced fragment due to fracture. [20,22]

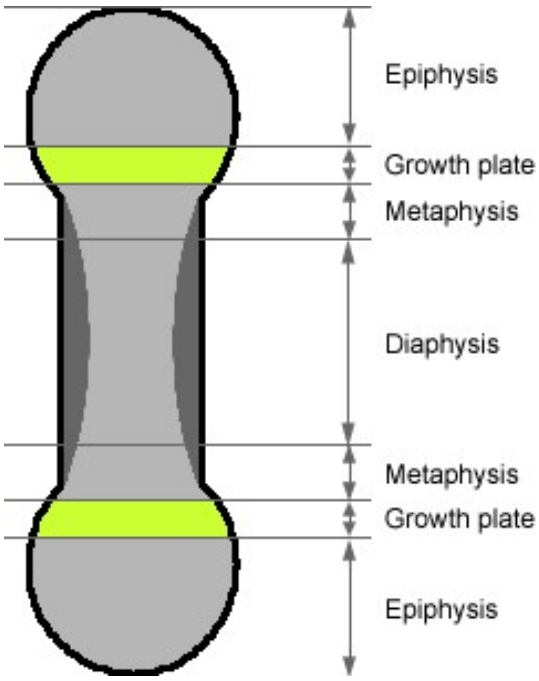

Figure 2: Components of a typical long bone during growth

2.1.2. Macrostructure of a Tubular Bone

As previously described, long bones of extremities are composed of the diaphysis, the epiphysis and the metaphysis. The diaphysis consists of a thick cylinder of compact bone (or cortical bone) with only a few trabeculae on its inner surface, whereas the epiphysis primarily consists of cancellous bone (synonyms are

lamellar, spongy, trabecular or medullary bone) enclosed by a thin layer of cortical bone. In addition, the epiphysis is covered by articular hyaline cartilage at its ends in order to form the synovial joint.

Macroscopically, cortical bone has a dense and solid texture, containing few spaces. This compact substance is of great importance in providing strength and rigidity and therefore in the reduction of stress caused by weight bearing and gravidity. In contrast, cancellous bone plays a more important role in metabolic functions. Its structure resembles a honeycomb pattern, consisting of an irregular lattice of osseous trabeculae with many large cavities between them. These cavities are filled with bone marrow, either red haematopoietic or yellow fat marrow, depending on the age and type of bone. The thick cortical bone of the diaphysis also encases a large marrow (or medullary) cavity where thin trabeculae are sparsely arranged. In adults, it mainly consists of fatty, yellow marrow that is not involved in haematopoiesis under normal circumstances. [15,19]

Each bone is enclosed in a connective tissue sheath - the periosteum - which is tethered to the underlying cortical bone by collagen fibres, termed Sharpey's fibres. The periosteal layer is absent from cartilaginous joint surfaces, sesamoid bone surfaces and the points of insertion of tendons and ligaments. Two distinct layers of the periosteum can be distinguished. The outer fibrous layer is composed of fibroblasts, collagen and elastin fibres. The inner osteogenic or cambium layer is highly cellular with mesenchymal progenitor cells, differentiated osteogenic progenitor cells, osteoblasts and fibroblasts. Both layers are traversed by a pronounced nerve and microvascular network. [19,23] The periosteum is highly active during bone development when it generates osteoblasts for appositional bone growth, and is also considered to be important in fracture healing. [19,23]

The endosteum, a thin membrane containing osteoprogenitor cells, bone-lining cells, osteoblasts, osteoclasts and reticular type III collagen fibres, lines the medullary cavity and covers the surface of the trabeculae of spongy bone. This inner surface of tubular bones is considered to be important in calcium homeostasis and acts as a reservoir of new bone-forming cells for remodelling and repair. [19]

2.1.3. Microstructure of a Tubular Bone

The Haversian systems or osteons are the functional units of compact bones and can reach a length of up to 1 cm and a thickness of up to 250 to 350 µm. [24] In the centre of such an osteon, the Haversian canal runs longitudinally and contains blood vessels, lymphatic vessels and nerves. The central canal is surrounded by between 5 and 20 concentric lamellar systems (special lamellae), composed of osteocytes and mineralised extracellular matrix whose collagen fibres run in circular branching bundles. Osteocytes derive from osteoblasts which have cemented themselves into the extracellular matrix that they have synthesised. These types of mature bone cell represent the main cellular component of cortical bone [14] and occupy spaces (lacunae) within the mineralised matrix. They extend filopodial processes into adjacent osteocytes and keep in contact via gap junctions. This network of osteocytes is assumed to play a fundamental role in cell communication and to be important in functional bone adaptation to external stimuli. [14] Numerous, branched, 0.5 to 0.25 µm [19] wide channels called canaliculi extend from the lacunae of osteocytes. They are devoid of extracellular matrix but filled with extracellular fluid, contain the cytoplasmatic projections of osteocytes and provide a route for the exchange of nutrients, gases and waste products between osteocytes and blood vessels [19].
The Haversian canals are connected to each other as well as to vessels of the periosteum and medullary cavity by oblique and transverse Volkmann canals. Remnants of circumferential lamellae of older and partially degraded bone tubules lie between osteons and constitute the interstitial lamellae. Each lamellar system is circumscribed by the so-called cement line, where the ground substance is composed of few collagen fibrils [24] but instead contains many glycoproteins and proteoglycans [19]. All osteons with their special lamellae and their interstitial lamellae are trapped by the outer and inner general lamellae [24] or external and internal circumferential lamellae [20]. They can be found adjacent to the periosteum and the endosteum, respectively, and are arranged parallel to the surface of the bone.

Spongy bone is not made up of actual osteons but of an irregular lattice of thin bony plates or spicules with a high surface-to-volume ratio. These trabeculae vary

in width and length and have many spaces which lie between the trabeculae and which are filled with bone marrow [15]. Since trabecular bone does not have an actual vascular supply, they receive their nutrients through diffusion from the adjacent medullary space. Hence a single trabecula does not exceed a thickness of about 200 to 300 µm [20], which is thought to be the maximum distance for possible diffusion.

2.1.4. Extracellular Matrix of Bone Tissue

In general, the extracellular matrix of every type of connective tissue is composed of ground substance and fibres. The extracellular matrix of bone tissue is a mineralised one, providing the characteristic hardness and rigidity of bones. In the early stages of bone formation, prior to mineralisation, the matrix is termed osteoid. The mineral portion of mature bones is predominantly composed of crystals of mineral salts which are present in the form of hydroxyapatite and mainly consist of calcium and phosphate hydroxide. [19] Inorganic mineral salts account for 50% of the overall extracellular matrix, organic matrix for 25%, and the remaining 25% are composed of water. [21] The organic matrix mainly consists of collagen fibres (95%) while the remaining organic component of 5% is made up of numerous non-collagenous proteins. [14] See also Figure 3.

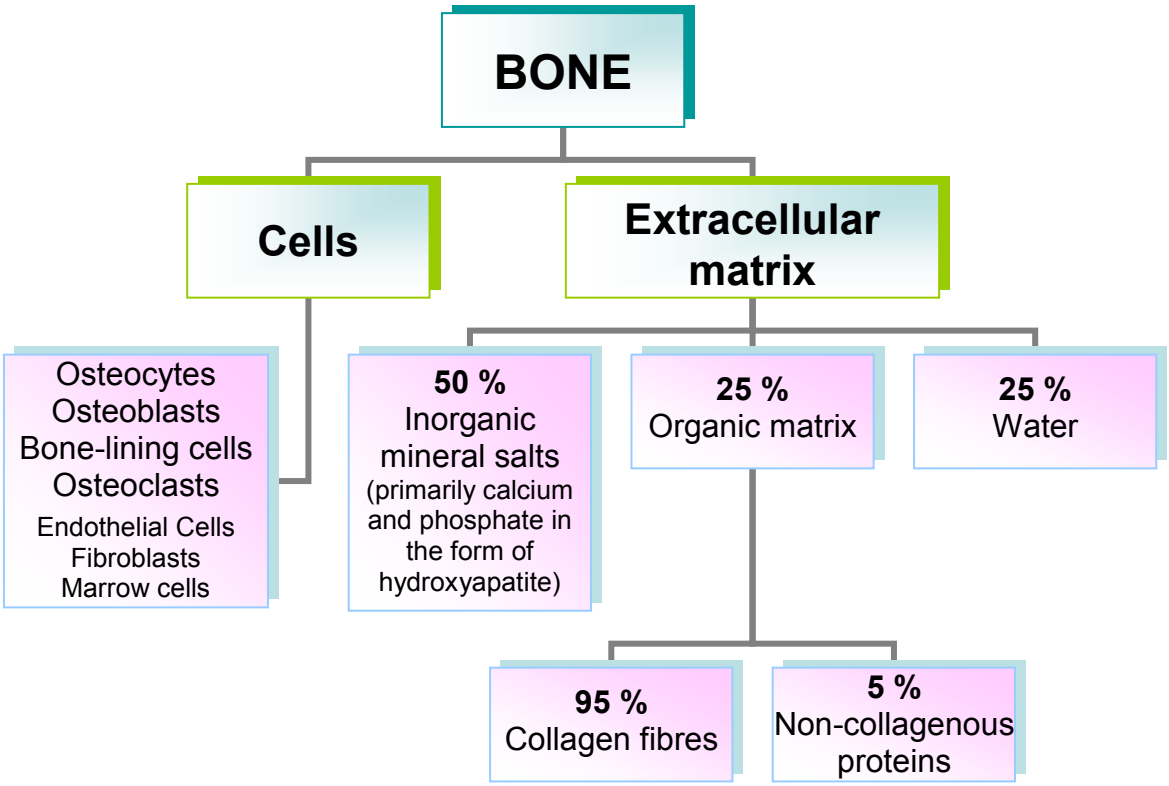

Figure 3: Components of bone tissue. Data out of [14,21].

2.1.4.1. Collagen

Collagen in bone is mainly type I, which is a banded (with 67 nm periodicity [14]), fibril-forming collagen. This triple-helical glycoprotein consists of three polypeptides bound tightly together. Two of these are identical α1 monomers encoded by the same gene, and one is an α2 monomer encoded by a different gene. [16] The collagen fibrils are stabilised by cross-links within fibrils and fibres. [18]

Collagen fibres are synthesised in the rough endoplasmic reticulum of osteoblasts. Polypeptide chains, which are rich in the amino acids proline and lysine, assemble into triple α-helices. After carbohydration and glycosylation in Golgi apparatus, these molecules are secreted as procollagen into the extracellular space. There, terminal registration peptides, which prevent intracellular polymerisation, are cleaved and procollagen converts into tropocollagen. Tropocollagen polymerises extracellularly and becomes more cross-linked, finally resulting in the assembly of collagen fibres. [25]

In primary bone, collagen fibres form a complex of irregularly woven meshwork. [19] The higher proportion of osteocytes and this disorganised arrangement of collagen fibres are characteristics of non-lamellar woven or bundle bone. Whenever the need for fast bone formation arises, such as in the formation of fracture callus, woven bone is formed. Lamellar bone, with its regularly ordered collagen fibres, is built up more slowly. [26] Eventually, woven bone is replaced by lamellar bone with collagen fibres running parallel to each other in the same lamellar layer. In the alternating layer, fibres run in opposite directions, resembling plywood. Due to this highly ordered arrangement, collagen fibres greatly contribute to the tensile, compressive and shearing strength of bone. [19] Moreover, collagens form a microenvironment that favours apatite nucleation; thus, collagens are essential for bone mineralisation. [14] Collagen fibres form gaps between the ends of tropocollagen units where the formation of hydroxyapatite crystals is most probably initiated. Within the collagen fibres, the hydroxyapatite crystals are arranged with their long axes parallel to the collagen fibril axes. [19]

2.1.4.2. Non-collagenous Proteins

The main types of non-collagenous proteins found in the extracellular matrix of bones are proteoglycans (glycosaminoglycan-containing molecules), glycoproteins and gamma-carboxy glutamic acid-containing proteins (Gla proteins). [27] The glycoprotein osteonectin is synthesised by osteoblasts, binds tightly to hydroxyapatite and collagen fibres and may play a role in the initiation of hydroxyapatite crystallisation. Osteocalcin, secreted by osteoblasts at sites of new bone formation, is a member of the Gla protein family and avidly binds calcium and hydroxyapatite. The glycoproteins osteopontin, bone sialoprotein and thrombospondin provide assistance in the adhesion of osteoclasts to bone surfaces. Proteoglycans like decorin and biglycan may bind transforming growth factor-β (TGF-β). [19]

2.1.5. Cell Types of Bone Tissue

In addition to the extracellular mineralised matrix, bone tissue contains a number of different cell types including osteocytes, osteoblasts, bone-lining cells, osteoclasts, endothelial cells, fibroblasts and marrow cells (Figure 3). [14]

2.1.5.1. Osteoblasts and Bone-lining Cells

Osteoblasts are of mesenchymal origin and are responsible for bone formation. Together with osteoclasts, they are in charge of bone remodelling in order to maintain and alter bone mass and support calcium homeostasis. Osteoblasts originate from multipotential mesenchymal stem cells, which have the ability to differentiate themselves into tissue-specific cells such as osteoblasts, chondrocytes, adipocytes and myoblasts (Figure 4). The development of the progenitor cells into a specific cell lineage is associated with the loss of their pluripotency and is dependent on the presence of certain regulatory factors. [28] Concerning the osteoblast lineage, multipotential mesenchymal stem cells progress into osteoprogenitors and then into preosteoblasts before becoming mature osteoblasts. [29,30]

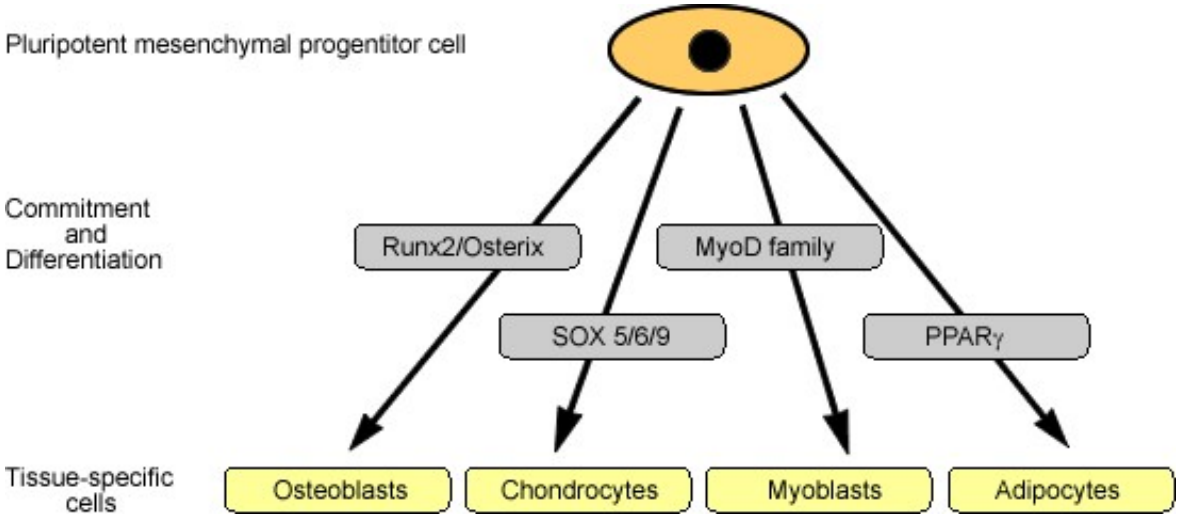

Figure 4: The development of tissue-specific cells from a pluripotent mesenchymal progenitor cell. Osteoblasts, chondrocytes, myoblasts and adipocytes derive from a common multipotential mesenchymal stem cell. Each different differentiation route depends on the presence of certain transcription factors including Runx2/Osterix, SOX5/6/9, MyoD family and PPARγ respectively. Modified after [28].

Bone morphogenetic proteins (BMPs) play a critical role in the commitment and differentiation of undifferentiated mesenchymal cells into osteogenic cells. [28] BMPs, except for BMP-1 (BMP-1 acts as a protease which cleaves the carboxy-

terminal propeptide from procollagen [31]), are growth factors and belong to the transforming growth factor-β superfamily. To date, 15 BMP family members have been identified. They regulate proliferation, differentiation and programmed cell death of cells in numerous tissues. However, the hallmark of BMPs is their ability to induce ectopic bone and cartilage formation. [32] BMPs are considered to be key regulators in the differentiation of osteoblasts and chondrocytes during skeletal development. [28] Signalling of BMPs is initiated upon their binding to transmembrane serine/threonine kinase receptors, which then proceed to phosphorylate and activate Smad transcription factors. Subsequently, the activated Smad proteins move into the nucleus and regulate the transcription of target genes. [32]
Runx2 (previously called core binding factor alpha 1, Cbfa1) and Osterix represent two other transcription factors which are absolutely required for osteoblast differentiation. It is suggested that they interact with Smad transcription factors. [28] Runx2 is expressed in mesenchymal condensations, osteoblasts and chondrocytes, and also plays a crucial role in inducing chondrocyte hypertrophy during endochondral ossification (specified below in 2.2). [33] Analysis of Osterix-null mice showed that Osterix acts downstream of Runx2. [28]

Osteoblasts are cuboidal mononuclear cells that can be found on the bone forming surfaces of growing or remodelling bone. In common with bone-lining cells, they build up a covering layer on the surfaces of trabeculae in the cancellous bone. [14,19] Osteoblasts synthesise numerous components of bone matrix including type I collagen, the non-collagenous proteins osteonectin, osteopontin, bone sialoprotein and osteocalcin, as well as alkaline phospatase [29]. Furthermore they express receptors for parathyroid hormone, 1,25-dihydroxycholecalciferol, estrogen and glucocorticoids [14] and promote mineralisation of the osteoid by transferring calcium and phosphate from intracellular vesicles into the extracellular space by means of exocytosis. The local extracellular concentrations of calcium and phosphate rise; consequently, crystal formation and growth are facilitated. [18]

Bone-lining cells are flattened epithelioid cells which are considered to be synthetically inactive osteoblasts. They cover bone surfaces where no significant remodelling takes place. They are present on the endosteal and periosteal surface

and line vascular channels within osteons. [19] Under certain circumstances they are capable of reverting into their previous osteoblastic phenotypes [34]; periosteal cells also possess this capacity. [35]

2.1.5.2. Osteocytes

Osteocytes, the most numerous cell type in bone tissue, are derived from osteoblasts which have encased themselves in their bone matrix. Osteocytes are of an ellipsoid cell shape and lie in lacunae within the mineralised matrix with their long axis parallel to lamellae. Their cytoplasm contains only a few organelles showing that their synthetical activity is highly reduced. [19]

Osteocytes remain in contact with adjacent osteocytes as well as with osteoblasts, bone-lining cells and the pericytes of capillaries and sinusoids, by gap junctions and numerous extending processes running in canaliculi. Communication also occurs through osteocyte expression of various signalling molecules such as prostaglandins and nitric oxide. The level of expression is influenced by mechanical strain. [26] Furthermore, osteocytes are capable of generating the protein osteopontin, which causes osteoblasts and osteoclasts to attach to the bone matrix. [36] Apoptosis of osteocytes can be initiated at either very high or very low mechanical strain levels and might be triggered by estrogen suppression. Apoptotic osteocytes generate signals which target and stimulate osteoclasts. [26] Thus, osteocytes play an essential role in the maintenance of bone mass and the adaptation of bone to mechanical strain patterns.

2.1.5.3. Osteoclasts

Osteoclasts play an important role in bone remodelling and are responsible for the resorption of bone tissue. They form resorption pits which are proceedingly filled up with new bone matrix synthesised by osteoblasts.

Osteoclasts are of haematopoietic origin and are suggested to derive from precursor cells found in the monocytes-macrophages lineage. [37,38] They are multinucleated giant cells with an average of 10 to 20 nuclei per cell, and lie tightly against the bone surface in resorption bays, termed Howship's-lacunae.

Resorption and degradation of mineralised bone matrix occur through the creation of an isolated acidic microenvironment between the osteoclast and the bone. The

edges of the osteoclast are therefore attached to the bone via transmembrane glycoproteins, termed integrins, which possess a vitronection receptor. The receptor recognises ligands with an arginine-glycine-aspartic acid motif which is found in a number of matrix proteins, such as osteopontin and bone sialoprotein. [38,39] This so called sealing zone isolates the resorptive acidified microenvironment from the general extracellular space. (Figure 5)

The characteristic feature of osteoclasts is the unique ruffled border of the plasma membrane where it joins the bone, which consists of numerous finger-like cytoplasmatic projections and contains a series of proton pumps. The osteoclast secretes proteolytic enzymes and hydrogen ions across its ruffled border membrane and into the isolated bone-resorbing compartment. The acidic environment (approximately pH 4.0) beneath the ruffled border dissolves bone minerals, while the proteases break down the matrix proteins. The products of digestion are then absorbed by the osteoclast, transcytosed in vesicles to the free surface of the cell, and released into the interstitial fluid. [16,18,38,40]

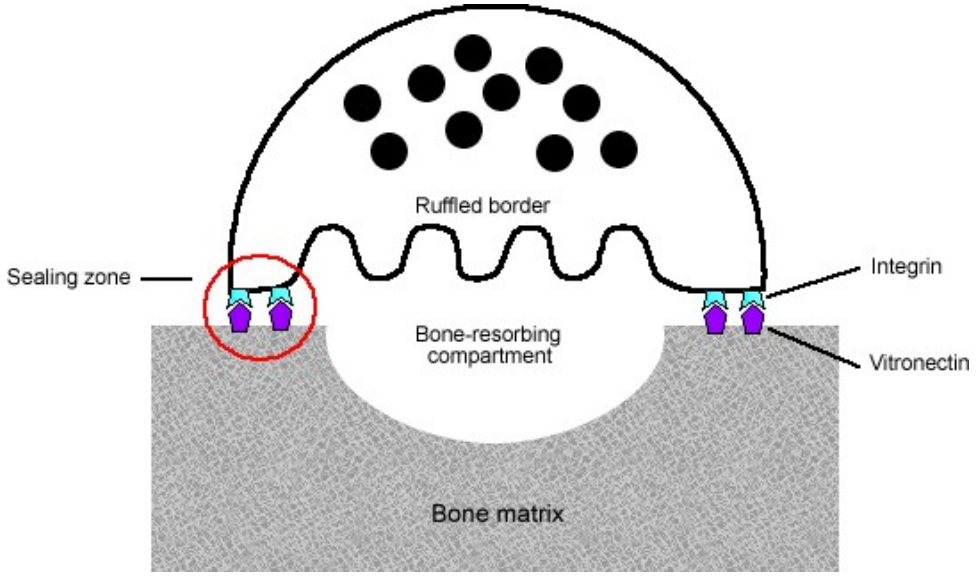

Figure 5: Bone resorption by the osteoclast. The edges of the multinucleated cell are tightly sealed to the bone, enclosing an isolated bone-resorbing compartment.

Various stimulators, leading to both the differentiation of osteoclast progenitors into osteoclasts and the activation of mature osteoclasts, have been described.

The mechanism of osteoclastogenesis depends mainly on receptor activator nuclear factor κB (NF- κB) ligand (RANKL) and macrophage-colony stimulating factor (M-CSF, also called CSF-1, colony stimulation factor-1). RANKL and M-CSF are secreted by osteoblasts and stromal cells and play a decisive role in osteoclast formation. As shown in Figure 6, RANKL binds and stimulates the transmembrane signalling receptor RANK (receptor activator nuclear factor κB), a member of the TNF receptor family to be found on osteoclast progenitors and osteoclasts. This RANKL-RANK interaction is involved in both the differentiation and the activation of osteoclasts. Because osteoblasts and stromal cells express RANKL as a membrane associated factor, cell-cell contact between osteoblasts/stromal cells and osteoclasts is necessary for the induction of osteoclastogenesis and osteoclast activation. The expression of RANKL in osteoblasts and stromal cells is upregulated by osteotropic hormones and factors like 1,25-dihydroxycholecalciferol, PTH, inflammatory cytokines like TNF-α and interleukins (IL-1, 6, 11, 17), PGE_2 and glucocorticoids. Osteoblasts also produce osteoprotegerin (OPG), a soluble decoy receptor that binds to RANKL. OPG competes with RANK on osteoclasts for RANKL binding and consequently inhibits osteoclast formation and activation. Thus, osteoblasts are capable of both inhibiting and enhancing osteoclast bone resorption by controlling the expression level of RANKL and OPG. [17,28,41,42]

Furthermore, TGF-β super family members like TGF-β and BMP-2 stimulate osteoclastogenesis in the presence of RANKL and/or M-CSF. Lipopolysaccharide and inflammatory cytokines such as TNF-α and IL-1 are directly involved in osteoclast differentiation and function through a mechanism independent of RANKL-RANK interaction. [28]

The transcription factor PU.1 acts early in osteoclastogenesis and regulates the initial stage of myeloid differentiation. PU.1 deficient mice lack osteoclasts and macrophages, but not monocytic cells. [21,28,33]

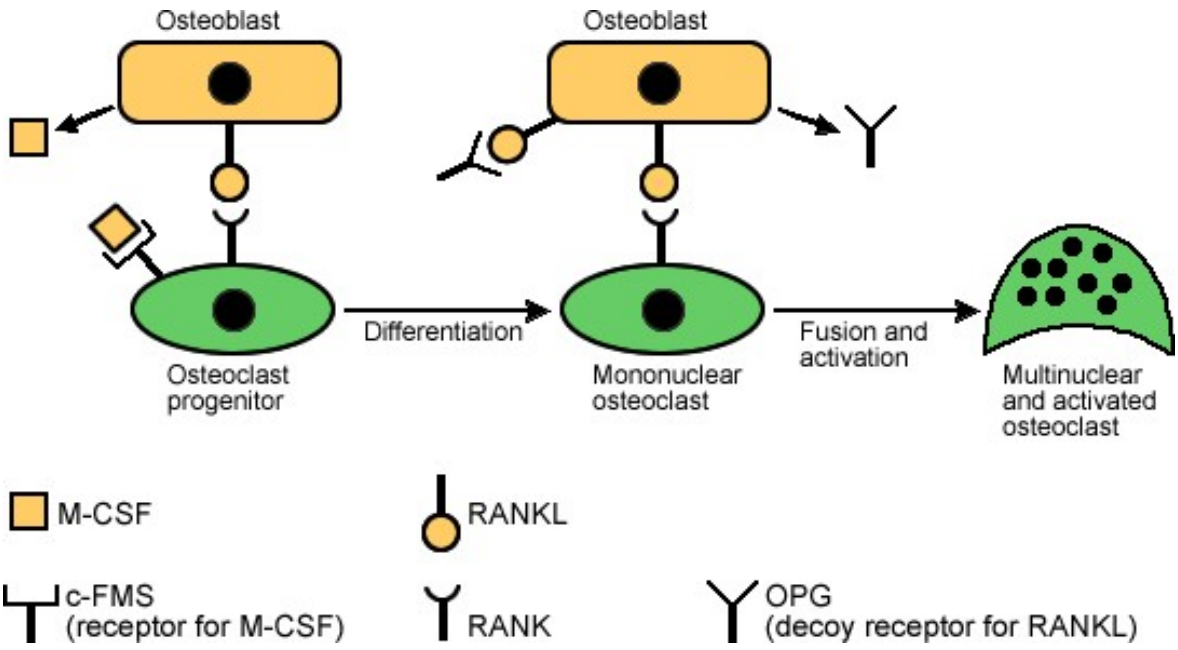

Figure 6: The regulation of osteoclast differentiation and activation by osteoblasts.

2.2. Long Bone Development and Growth

Bone formation requires epithelial-mesenchymal interaction, condensation and differentiation [17] and is initiated by the condensation of mesenchymal cells in the early embryonic phase. In the case of the development of long bones, two upper and two lower limb buds are formed, containing undifferentiated mesenchymal cells and an apical ectodermal ridge at the distal margin of each limb bud. Mesenchymal cells, which are primarily distributed uniformly across the limb buds, start to condensate, adopting the shape of the skeletal elements. [43]

Mesenchymal condensations lead to chondrogenesis and osteogenesis, respectively, depending on the type of bone and the associated kind of ossification. [17] The process of bone formation can be distinguished into intramembranous and endochondral ossification. Several bones such as flat bones and some facial bones develop through intramembranous ossification which means that condensed mesenchymal cells differentiate directly into bone-forming osteoblasts. In contrast, endochondral ossification involves the formation of hyaline cartilage templates which are then replaced by bone. In this case,

mesenchymal cells convert into chondroblasts and chondrocytes which start to produce a hyaline cartilage model surrounded by a condensed, vascular, bilaminar mesenchyme, termed the perichondrium. The outer layer of the perichondrium consists of fibroblasts, whereas the inner layer contains osteogenic precursor cells.

2.2.1. Cartilage Cells and Matrix

Chondrocytes are the principle cell type in cartilage and occupy small lacunae in the matrix that they secrete. Chondrocyte precursor cells - which have the ability to proliferate as well as to synthesise cartilage matrix rich in collagen type I, hyaluronan, tenascin and fibronection - are termed chondroblasts. As they mature, they become rounded chondrocytes, lose their ability to divide and secrete collagen type II, as well as collagen type IX and type XI, Gla protein, aggrecan and link protein. [14,17] However, the term “chondrocyte” is more frequently used to describe both cell types (chondroblasts and chondrocytes).

The DNA-binding protein and transcription factor SOX9 is essential for converting mesenchymal stem cells into chondrocytes (see also Figure 4), for further differentiation and maturation of chondrocytes, and for the stimulation of the transcription of a series of cartilage matrix genes such as collagen type II, type IX, and type XI and aggrecan. It binds to specific enhancer regions in the promoters of these target genes in order to activate gene transcription. SOX9 is expressed in cells of mesenchymal condensations as well as in proliferating chondrocytes, but not in hypertrophic chondrocytes. Moreover, other SOX-family members such as SOX5 and SOX6 cooperate with SOX9. [17,21,44,45]

The extracellular matrix of hyaline cartilage, which is synthesised by chondrogenic cells, is mostly made up of collagens and proteoglycans, but also of non-collagenous proteins. Collagen type II is specific to cartilage and is the major type of collagen present in cartilaginous tissue. It is a homotrimer of 3 identical type II α1-chains. Type IX and type XI collagens are present in relatively small amounts. All 3 types of collagen form a heterotypic fibril, with type II collagens surrounding a type XI core filament. Type IX collagen is deposited on the surface, prevents

further growth in fibril diameter and mediates the interaction of type II collagen with other extracellular matrix components. When chondrocytes mature into hypertrophic chondrocytes (see below), they secrete collagen type X, a short chain homotrimeric collagen molecule. [14,45,46]

Proteoglycans, the other major type of cartilage matrix molecule, consist of a core protein to which glycosaminoglycan side-chains - such as chondroitin sulphate, dermatan sulphate, heparin sulphate, keratin sulphate and hyaluronic acid - are attached. In cartilaginous matrix the following proteoglycan macromolecules are the major components: aggrecan, decorin, biglycan and fibromodulin. Aggrecan, the largest cartilage proteoglycan in terms of quantity, provides the osmotic properties necessary for cartilage to resist compressive loads. Collagen type II and aggrecan make up 90% of cartilage matrix.

Cartilage oligomeric matrix protein (COMP), fibronectin, link protein, tenascin-C, vitronectin and laminin are regarded as non-collagenous proteins. In cartilaginous matrix, they appear in small amounts and are responsible for cell-cell and cell-matrix interactions. [14,45,46]

2.2.2. Endochondral Ossification of Long Bones (Figure 7)

The cartilage scaffolds of long bones develop a primary centre of ossification early in foetal life. Therefore, chondrocytes in the middle part of the primitive shaft stop proliferating, accumulate glycogen, become hypertrophic, produce collagen type X and control the mineralisation of their surrounding matrix by the formation of matrix vesicles. [44] These matrix vesicles [45] are formed by budding of the chondrocyte's plasma membrane, and contain calcium as well as high concentrations of the enzyme alkaline phosphatase, expressed by hypertrophic chondrocytes. When released into the extracellular matrix, alkaline phosphatase increases the concentration of phosphate ions, which are necessary for the calcification process. Thus, matrix vesicles serve as a nidus for the mineralisation of the extracellular cartilage matrix. Matrix vesicles also contain matrix metalloproteinases (MMPs) expressed by hypertrophic chondrocytes. MMPs function as proteolytic enzymes, which are involved in the degradation of extracellular matrix proteins during endochondral ossification.

At the same time, cells in the inner layer of the perichondrium, which surrounds the cartilage template, differentiate themselves into osteoblasts and start to form a peripheral bone layer. This bone collar is formed by intramembranous ossification. It encloses the central shaft and is covered by periosteum (formerly perichondrium) on its outer surface.

In the meantime, hypertrophic chondrocytes produce vascular endothelial growth factor (VEGF) and attract chondroclasts that begin to digest parts of the mineralised cartilage matrix. In their final stage, hypertrophic chondrocytes undergo programmed cell death or apoptosis. VEGF and other angiogenic factors lead to the invasion of vascular osteogenic buds from the periosteum into the primary ossification centre. These osteogenic buds are blind-ended capillary sprouts and are accompanied by osteoprogenitor cells and osteoclasts. The mid-shaft mineralised cartilage that is left behind serves as a scaffold for osteoblasts, which now deposit osteoid, forming the primary spongiosa. It consists of internal mineralised cartilage tissue enclosed by bone tissue. Trabecular bone and the medullary cavity eventually develop through continuous erosion by osteoclasts as well as through osteoid deposition and bone formation by osteoblasts, whereas the bone collar increases in diameter and extends towards both ends of the shaft, becoming cortical bone. [19,21,25,44]

The procedure of endochondral bone formation proceeds in a centrifugal direction towards both ends of the diaphysis while chondrocytes continue to proliferate in order to further enlarge the cartilage model.

In tubular bones, shortly before birth or even during early childhood (depending on the type of bone), a secondary centre of ossification appears in their epiphyses in order to convert the epiphyseal cartilage into bone by means of endochondral ossification. The same events as described above take place. Almost all the cartilage of the epiphysis is replaced by bone, except for a specialised layer of articular hyaline cartilage which persists at the joint surface, and a horizontal zone entrapped between the metaphysis and the epiphysis termed the growth plate (or epiphyseal plate, cartilage plate, physis). [15,17,19]

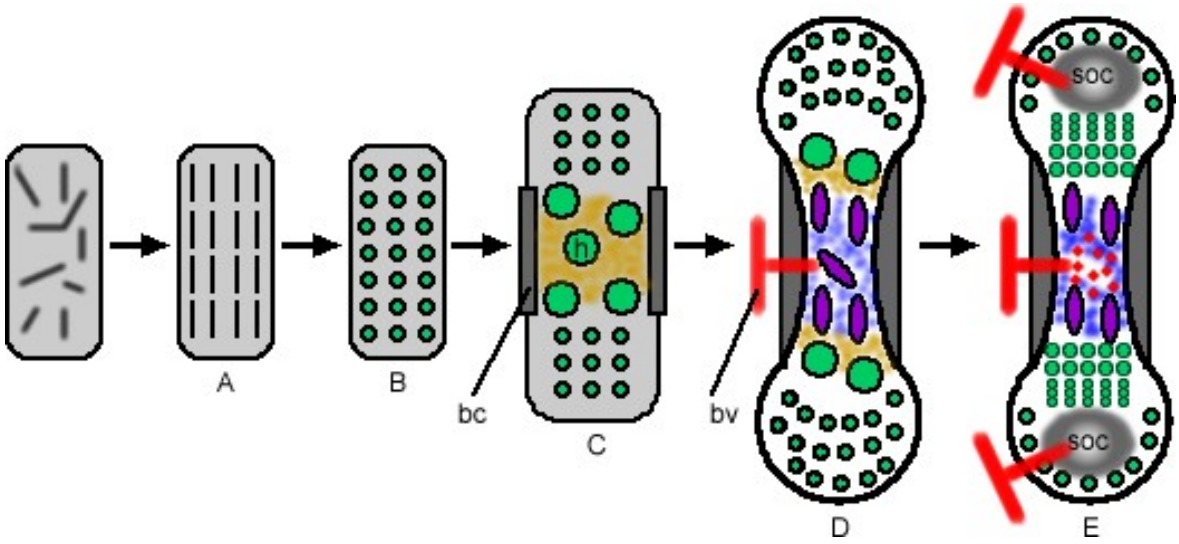

Figure 7: The stages of endochondral ossification in a long bone. *(A)* Mesenchymal condensation. *(B)* Cells of the condensation become chondrocytes and form the cartilage template. *(C)* Chondrocytes at the centre of the cartilage template stop proliferating, become hypertrophic (h) and control matrix calcification. Perichondrial cells adjacent to hypertrophic chondrocytes differentiate themselves into osteoblasts and form the bone collar (bc). *(D)* The ingrowth of blood vessels (bv) into the primary ossification centre is accompanied by the invasion of osteoblasts, which lay down primary bone onto calcified cartilage remnants. Chondrocytes continue to proliferate, therefore lengthening the bone. *(E)* A secondary ossification centre (soc) appears at both ends of the bone. The growth plate can be found below the secondary ossification centre. Haematopoietic marrow expands in the medullary cavity.

2.2.3. The Growth Plate (Figure 8)

After birth, the growth plate is responsible for longitudinal bone growth by means of endochondral ossification. The epiphyseal plate can be divided into several horizontal zones, marked by chondrocytes at different stages of differentiation. [45-47] At the epiphyseal end of the growth plate, the reserve zone (or germinal zone or resting zone) contains quiescent chondrocytes, which are also referred to as stem cells. This layer shows a high ratio of extracellular matrix to cell volume and is important for the orientation of chondrocytes of the underlying zone and therefore essential for unidirectional bone growth. [48] When the stem cells enter the proliferating zone (or proliferative zone), they show a flattened appearance, divide excessively, arrange in columns and synthesise large amounts of extracellular matrix proteins, mainly collagen type II and the proteoglycan

aggrecan. Forriol and Shapiro deviate slightly from this kind of zonal classification and refer to a columnar zone instead of a proliferating zone. They further divide this columnar zone into two well-defined areas, the upper proliferating zone where the flattened chondrocytes show multiple mitoses, and the lower maturation zone where the matrix synthesis occurs and chondrocytes contain a high amount of rough endoplasmic reticulum. [46] The columns of chondrocytes are arranged parallel to the longitudinal axis of the bone and are separated from each other by longitudinal septa of cartilage matrix. The number of cells in each column varies from 10 to 20, depending on the current mitotic activity of the column. Chondrocytes lose their ability to proliferate and start to mature into prehypertrophic and finally fully differentiated round hypertrophic chondrocytes. Therefore, they increase their intracellular volume between five and ten-fold. This kind of swelling reflects an active process and is achieved through a rise in the number of intracellular organelles and an intracellular accumulation of glycogen. Hypertrophic chondrocytes prepare the matrix for calcification and vascularisation. They stop to synthesise type II collagen and instead produce short-chain type X collagen and matrix vesicles, which function as the initial site of mineralisation in the hypertrophic region (see also 2.2.2). The mineralisation of the longitudinal septa of the cartilage matrix takes place in the zone of provisional calcification. Furthermore, hypertrophic chondrocytes secrete VEGF in order to stimulate the formation of blood vessels. Vascular ingrowth into the metaphyseal end of the growth plate (zone of vascular invasion) is essential for the invasion of osteoprogenitor cells, osteoblasts, chondroclasts and osteoclasts. Eventually, hypertrophic chondrocytes undergo apoptosis in the mineralised zone. The different stages of chondrocyte differentiation, starting with the germinal cell, continuing with the proliferating cell and the hypertrophic cell and resulting in the apoptotic cell, are completed within 24 hours. [45]

At the junction of the metaphysis and the epiphyseal plate, approximately 80% of the mineralised longitudinal septa are destroyed by chondroclasts, while the remaining longitudinal septa serve as templates onto which osteoblasts deposit bone matrix. Thus, primary spongiosa, which consists of a mixture of mineralised cartilage and bone tissue, is formed. These primary trabeculae undergo rapid remodelling through bone resorption by osteoclasts and bone formation by

osteoblasts. Gradually, all cartilaginous material is removed and secondary trabeculae appear. [45-47]

To summarise, bones gain length by means of matrix synthesis, cell proliferation and particularly through the mechanism of cell hypertrophy. [46]

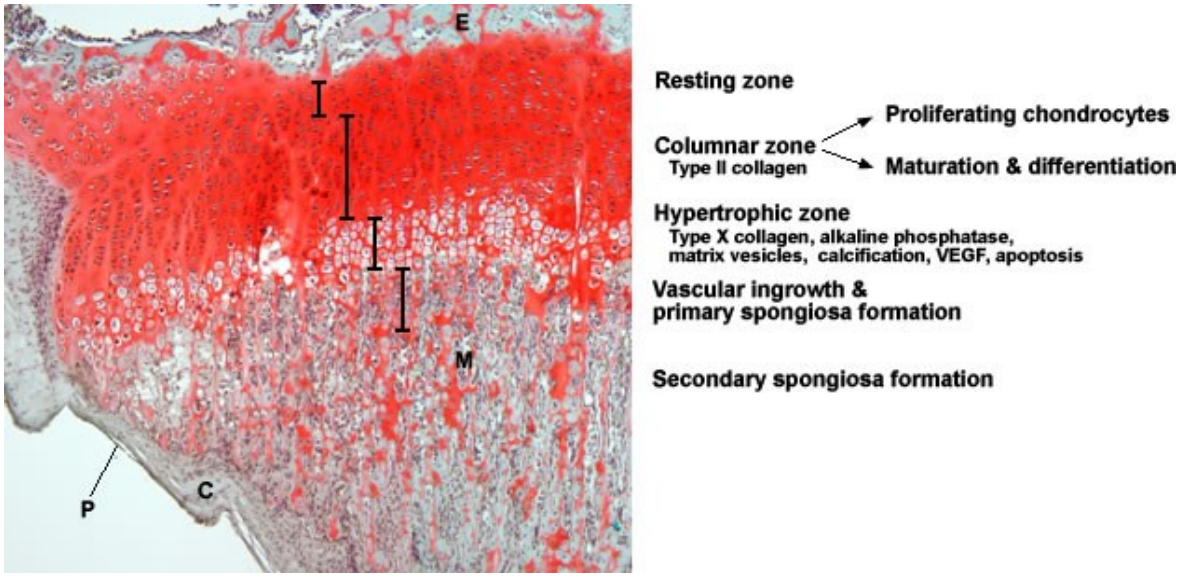

Figure 8: A section of the proximal growth plate of a rat tibia. The growth plate can be found between the epiphysis *(E)* and the metaphysis *(M)*. Several zones within the growth plate represent the life cycle of chondrocytes, which consists of proliferation, differentiation, hypertrophy and apoptosis. (For details see text above.) Generally, bone consists of cancellous and cortical bone *(C)* and is enclosed by the periosteum *(P)*. Safranin-O staining. Light microscopy. (Friendly provided by Dr. Gregor Janeciz.)

The periphery of the epiphyseal plate is surrounded by a ring whose fibres are arranged in vertical, circumferential and oblique directions. The ossification groove of Ranvier contains chondrocyte progenitor cells which contribute to the latitudinal growth of the epiphyseal plate. The perichondrial fibrous ring of LaCroix merges with the periosteum of the bone and mechanically supports the physis in case of compression, tension or shear loads. [45] Both the periosteum and the perichondrial ring are firmly anchored to the epiphysis.

In human adolescents, growth plates disappear after growth has finished. The height of the proliferating and hypertrophic zones decreases, leading to vascular

anastomoses between the metaphyseal and epiphyseal vessels and the formation of bone bridges. Eventually, growth is terminated by the fusion of the epiphysis to the metaphysis. Physeal closure occurs at different times, depending on its location within the bone and on the specific bone in which it takes place; even one individual growth plate does not show simultaneous closure across its entire width. Physeal fusion starts about 2 years earlier in girls than in boys. [46]

2.2.4. Vascular Supply of the Physis

The avascular epiphyseal plate is supplied by epiphyseal and metaphyseal vessels. The resting zone, proliferating zone and upper hypertrophic zone receive oxygen and nutrients from epiphyseal vessels by means of diffusion. The final 3 to 4 rows of hypertrophic cells are nourished by metaphyseal vessels which invade the lowermost part of the hypertrophic zone. Transphyseal anastomoses between metaphyseal and epiphyseal vessels never physiologically appear during growth. Abnormal vascular anastomoses would cause the formation of pathological bone bridges. Damage to the epiphyseal vascularisation can result in premature physeal closure, whereas injury to the metaphyseal vessels gives rise to a temporary increase in the height of the growth plate. This occurs because the matrix in the lower regions of the hypertrophic zone cannot calcify and hypertrophic chondrocytes accumulate. [46]

Generally speaking, long bones are supplied by the nutrient artery, the periosteal arteries and the metaphyseal and epiphyseal arteries. The nutrient artery, which branches off from a systemic artery, enters the diaphyseal shaft through nutrient foramina leading into nutrient canals. In the medullary cavity, this main artery divides into ascending and descending arteries which further divide into cortical branches, supplying the endosteum and diaphysis, as well as into medullary arteries which form a mesh of medullary sinusoids. [15,19]
Periosteal plexuses derive from arteries of neighbouring muscles and nourish the outermost osteons of the cortical bone. Epiphyseal arteries branch off from neighbouring systemic vessels, whereas metaphyseal arteries fork from periarticular vascular arcades. [19]

2.2.5. Growth of Bone Diameter

Radial bone growth plays an important role in the stabilisation and strengthening of bones as they become increasingly longer. Radial bone growth occurs through the direct apposition of cortical bone by osteoblasts which dwell in the inner cambium layer of the periosteum. This periosteal apposition is coordinated with the erosion of bone by osteoclasts on the endocortical surface in order to maintain the just dimensions of the medullary cavity. Consequently, the cortex is displaced farther and farther from the neutral axis. Androgen and growth hormone stimulate periosteal apposition, whereas estrogen inhibits it. [47,49]

2.2.6. Regulation of Longitudinal Growth at the Growth Plate

The control of longitudinal bone growth occurs at three different levels: Firstly extrinsic factors such as hormones provide systemic control. Secondly intrinsic molecules provide local regulation of growth. (Figure 9) And thirdly mechanical forces also influence bone growth. [47]

With regards to the effects of mechanical forces on bone growth, Rauch summarised that mild tension and mild compression would increase growth, whereas severe compression would inhibit it. [47] He therefore slightly altered the Hueter-Volkmann law of the 19th century which proclaimed that compression inhibited bone growth. [50]

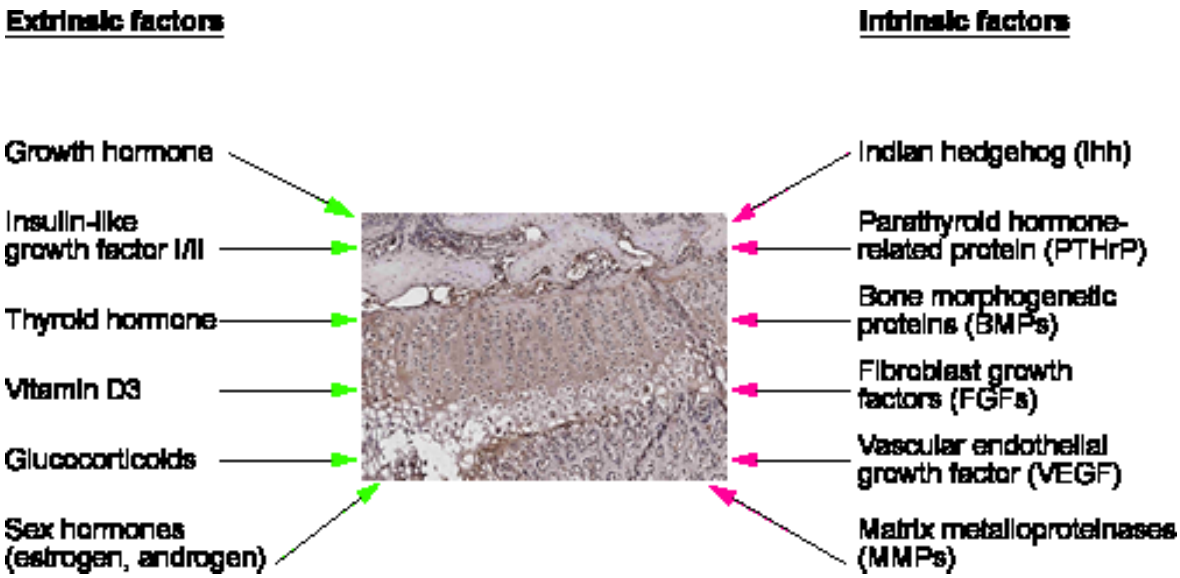

Figure 9: Major extrinsic and intrinsic molecules controlling the growth plate. [46]

2.2.6.1. Major Intrinsic Molecules

Bone morphogenetic proteins (BMPs) (see also 2.1.5.1) play important roles at every stage of endochondral bone formation. Early in the development of limb buds, they are critical in the formation of mesenchymal condensations. In long bones, BMP2, -3, -4, -5 and -7 are expressed in the perichondrium, BMP2 and 6 are synthesised by hypertrophic chondrocytes and BMP7 is also found in proliferative chondrocytes. BMPs have a positive effect on the proliferation of chondrocytes and therefore increase the length of proliferating columns. Furthermore, they delay the terminal differentiation of hypertrophic chondrocytes and increase the expression of Ihh by prehypertrophic chondrocytes. [44,46,51] (Figure 10)

The binding of fibroblast growth factors (FGFs) to fibroblast growth factor receptors (FGFRs), a family of four major transmembrane tyrosine kinase receptors, affects chondrocyte proliferation and differentiation. FGF signalling (especially the stimulation of FGFR3) negatively regulates chondrocyte proliferation, accelerates terminal differentiation of hypertrophic chondrocytes, suppresses Ihh expression and shortens proliferative columns. [44,51] FGFs therefore act antagonistically to BMPs at each level. (Figure 10)

Indian hedgehog (Ihh) belongs to the hedgehog family and is similar to Sonic hedgehog, which is critical for embryonic patterning and limb bud formation. Ihh is synthesised by prehypertrophic and early hypertrophic chondrocytes. The binding to its receptor Patched-1 (Ptch1) leads to the activation of the transmembrane protein Smoothened (Smo), which further triggers an intracellular signal cascade resulting in gene expression, including the expression of ptch1. [52] Ihh directly stimulates chondrocyte proliferation. Moreover, Ihh delays chondrocyte hypertrophy but only in a PTHrP dependent manner.

The auto/paracrine factor parathyroid hormone-related peptide (PTHrP) is synthesised by a series of adult and foetal tissues. PTHrP binds to and activates the same G-protein-coupled receptor that is used by the calcium-regulating hormone PTH. In the growth plate, these PTH/PTHrP receptors are expressed at low levels by proliferating chondrocytes and at high levels by prehypertrophic chondrocytes. PTHrP is synthesised by perichondrial cells and chondrocytes in the periarticular region of long bones. PTHrP signalling inhibits the further maturation of proliferating and prehypertrophic chondrocytes and keeps the proliferating chondrocytes in the proliferative pool. [44,45,51]

The interaction of Ihh and PTHrP can be described as a negative-feedback loop. PTHrP acts on the receptor of proliferating chondrocytes in order to keep them proliferating. Thus, PTHrP represses the production of Ihh by pre-/hypertrophic chondrocytes by delaying hypertrophy. When the proliferating chondrocytes are no longer sufficiently stimulated by PTHrP, they become hypertrophic and start to secrete Ihh. In response, Ihh stimulates the proliferation of chondrocytes and increases the production of PTHrP by cells of the periarticular region. [44,45,51] (Figure 10)

Vascular endothelial growth factor (VEGF) is absolutely necessary for the ingrowth of new vessels into the growth plate. It is synthesised by hypertrophic chondrocytes, but is not expressed by resting and proliferating chondrocytes. VEGF targets vascular endothelial cells and stimulates their proliferation, migration and finally the formation of blood vessels. It may be speculated that VEGF also possesses an autocrine role since the receptor for VEGF has been found on hypertrophic chondrocytes. However, it is not clear how VEGF directly affects chondrocytes. [45,46]

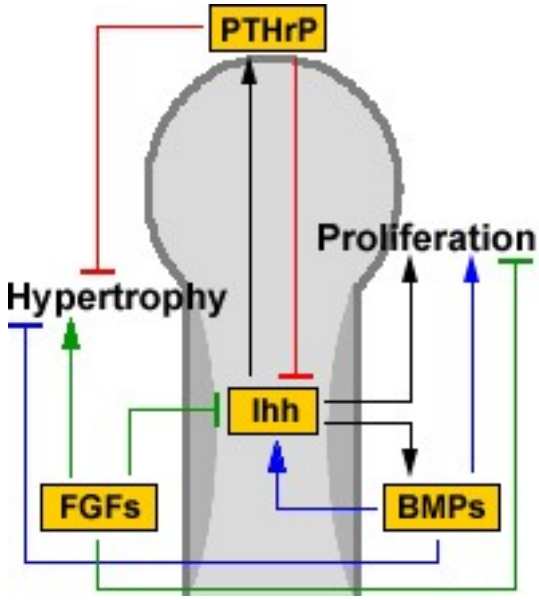

Figure 10: Schematic model of feedback loops and biological activities of Ihh, PTHrP, FGFs and BMPs in the growth plate.

2.3. Fracture Healing

Fracture healing describes a complex, highly orchestrated and multistage biological process that requires the coordinated interaction of vascular cells, skeletal precursor cells as well as immune and haematopoietic cells within bone marrow. Bone is one of the few tissues in the body that responds to injury with the reestablishment of the pre-existing tissue without resulting in the formation of a poorly organised scar. Both the original geometry and biomechanical properties are largely restored. [53-55]

During the process of fracture repair, specific pathways of embryological skeletal development and skeletal growth are recapitulated. Four major components contribute to the healing process: the periosteum, the cortical bone, the bone marrow and the external soft tissue surrounding the fracture site. [53,56] The level of contribution from each individual tissue varies and is dependent on several factors concerning the injured tissue, for instance the mobility of the fracture site,

age, oxygen tension, nutrients, pH, extent of injury to hard and soft tissue and level of growth factors and hormones. [55,57]

Two types of fracture healing can be distinguished: direct or primary cortical fracture healing and indirect or secondary fracture healing. The former describes the direct ingrowth of Haversian systems across the fracture without the previous formation of callus and occurs only when anatomic reduction and rigid immobilisation are warranted, for example by means of an internal fixation. The cortex functions as the major participant in this process, whereas the periosteum, the bone marrow and the external soft tissues are little or not involved.
Secondary fracture healing is characterised by the formation of a fracture callus and the occurrence of both endochondral and intramembranous ossification. It is the result of the incidence of micromotions at the fracture site. Such mircomotions enhance periosteal response and hence the process of callus formation, whereas rigid fixation inhibits callus generation. Worldwide most fractures remain untreated or are left without a rigid fixation; this means that the majority of fractures heal by secondary regeneration process. [53,55]

2.3.1. Fracture Repair Sequence

The following describes the distinct stages of secondary fracture healing.
Immediately after the initiation of bone injury, a haematoma appears within the fracture gap and an inflammatory response takes place. The haematoma contains numerous leukocytes, macrophages and lymphocytes which secrete important proinflammatory cytokines. Within 24 hours after fracture, the periosteum adjacent to the fracture site reacts through an increased proliferation of osteogenic precursor cells which then differentiate into bone-forming osteoblasts. Osteoblasts start with the formation of woven bone through intramembranous ossification. Hard callus appears under the periosteal cambium of both fractured ends of the bone. The intensified proliferation rate in the inner layer of the periosteum stops within two weeks, indicating the reduction of periosteal response. [53,56]
Furthermore, the first 7 to 10 days of fracture repair involve the formation of cartilage termed soft callus which serves as a bridging callus by overlying the fracture site. The origin of the cells that are responsible for this endochondral

cartilage formation is not been, until now, fully elucidated. Gerstenfeld and collaborators discussed that either the local periosteum, the surrounding muscle tissues or the marrow space provide mesenchymal stem cells and chondrogenic precursor cells which then become chondroblasts. [58]

Consequently, by the middle of the second week of fracture repair, hard callus, which is the result of intramembranous ossification, as well as soft callus, which develops through endochondral ossification and stabilises the fracture fragments, can be found at the fracture site. [53,56]

Chondrocytes of the soft callus start to mature into hypertrophic cells in order to prepare the extracellular matrix for calcification. Approximately two weeks after fracture hypertrophic chondrocytes become the main cell type in the chondroid callus and the first few areas begin to calcify. After 5 or 6 weeks almost the entire callus is composed of calcified cartilage which is then resorbed by multinucleated chondroclasts. Blood vessels penetrate the tissue and allow the invasion of mesenchymal stem cells that differentiate into osteoprogenitor cells and then into osteoblasts. Six to seven weeks post-fracture the callus consists of calcified cartilage and newly formed woven bone. Remodelling by osteoclasts and osteoblasts finally enables the conversion into lamellar bone. [53,56]

Lee and colleagues hypothesised that the removal of hypertrophic chondrocytes during endochondral fracture healing is the result of a genetically programmed process resulting in apoptotic cell death. [59]

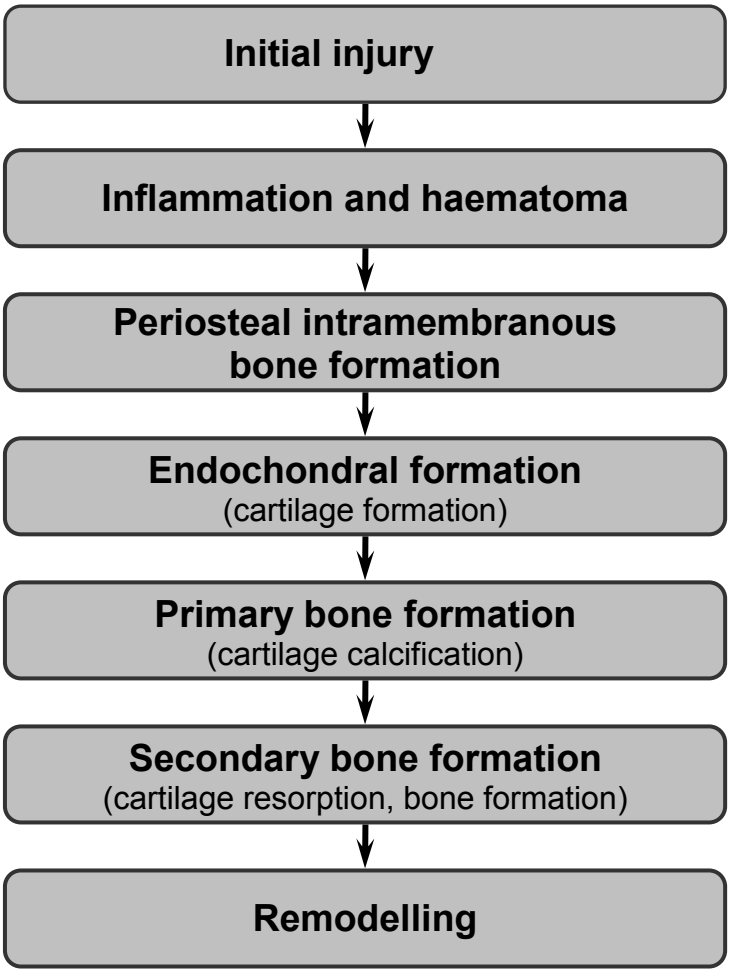

Figure 11: Different stages of secondary fracture healing.

2.3.2. Molecular Control of Fracture Healing

Multiple factors regulate the series of complex events during bone repair. Although the regulatory pathways are not yet fully elucidated, three groups of soluable factors are considered to act as the main regulators in fracture healing: (1) proinflammatory cytokines, (2) members of the TGF-β superfamily and (3) metalloproteinases and angiogenic factors. [58]

2.3.2.1. Proinflammatory Cytokines

The activation of the immune system and the expression of cytokines initiate the process of fracture repair during the initial inflammatory phase which immediately follows bone injury. [60] The proinflammatory cytokines interleukin 1 (IL-1),

interleukin 6 (IL-6) and tumor necrosis factor α (TNF-α) are secreted by macrophages, inflammatory cells as well as mesenchymal and osteoblastic cells present in the periosteum. They are critical for chemotaxis of other inflammatory cells, the enhancement of extracellular matrix production and the stimulation of angiogenesis. [61] Two expression peaks can be recognised: The first appears within 24 hours post-fracture and the second at a very late stage of bone repair, namely during the phase of bone remodelling. Between these two peaks their expression is reduced to very low levels. [55,61]

TNF-α takes up an unusual position among the above mentioned inflammatory cytokines as it is also expressed at high levels in hypertrophic chondrocytes [61] and shows an additional peak of expression at the end of the period of cartilage resorption. [54,58] TNF-α greatly promotes the process of fracture healing; as Gerstenfeld and co-workers demonstrated, the absence of TNF-α signalling in receptor deficient mice leads to a delay of endochondral tissue resorption, resulting in the inhibition of new bone formation. [62] TNF-α participates in the recruitment of mesenchymal stem cells, stimulates apoptosis of hypertrophic chondrocytes and elevates the function of osteoclasts. [62]

Fracture repair involves two types of resorption. The first takes place at the end of the endochondral period when mineralised cartilage is eroded and primary bone is formed. The second type occurs during the phase of remodelling and formation of secondary bone. While the second type of resorption seems to be dependent on the activities of IL-1, IL-6 and TNF-α, the first type of resorption shows elevated levels of M-CSF, RANKL and OPG. Consequently, Gerstenfeld and collaborators concluded that the mechanisms which regulate cartilage resorption are different from those which regulate bone resorption during the remodelling phase. [58]

2.3.2.2. Transforming Growth Factor β Superfamily

The TGF-β superfamily is a large group of structurally and functionally related polypeptides consisting of at least 34 distinct growth and differentiation factors. [55] Specific members of this superfamily are actively involved in fracture healing, such as bone morphogenetic proteins (BMPs 1-8), growth and differentiation factors (GDF-1, 5, 8, 10) and transforming growth factors (TGF-β1, β2, β3). In

spite of their structural and functional relation to each other, each type shows a distinct temporal expression pattern (Figure 12) and has a unique role during the different stages of intramembranous and endochondral bone ossification of fracture repair. [63] For instance, BMPs (see also 2.1.5.1 and 2.2.6.1) are synthesised by osteoprogenitors, mesenchymal cells, osteoblasts and chondrocytes, and primarily regulate the differentiation of mesenchymal stem cells into the osteogenic and chondrogenic lineages. Moreover, they promote the terminal differentiation of committed osteogenic and chondrogenic cells, stimulate angiogenesis, control the synthesis of extracellular matrix and enhance the synthesis of VEGF and IGF. [55] However, up till now it has been difficult to define the specific functional role of many of the members of this superfamily as these factors seem to have overlapping which act as part of a network.

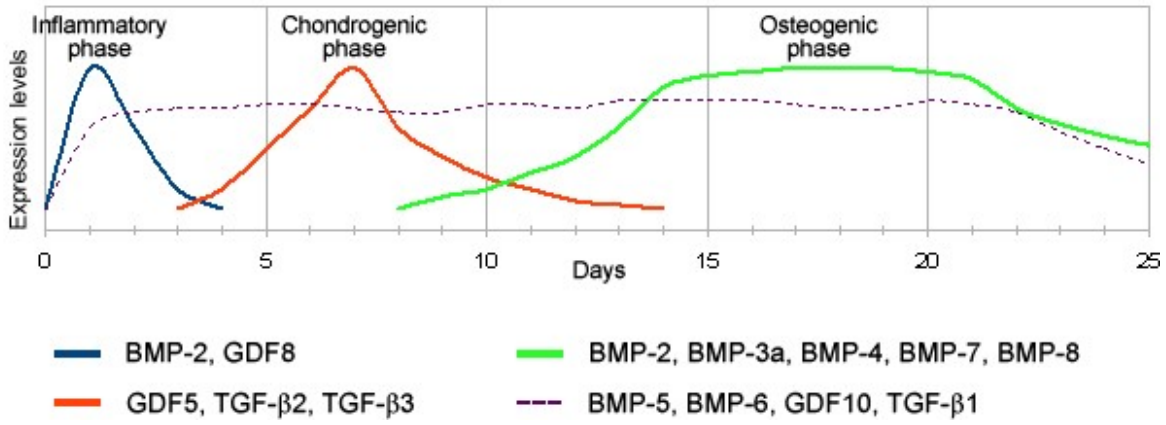

Figure 12: Schematic summary of the temporal expression patterns of TGF-β superfamily members during animal fracture healing. BMP-2 and GDF8 show maximal expression on day 1 after fracture, BMP-2 shows another elevation during the osteogenic phase. GDF5, TGF-β2, and TGF-β3 are maximally expressed 7 days after fracture, suggesting their potential role for cartilage formation. The expression of BMP-3a, BMP4, BMP-7 and BMP-8 occurs mainly from day 14 until day 21 post-fracture during the period of cartilage resorption and bone formation. BMP-5, BMP-6, GDF10 (or BMP-3b) and TGF-β1 show elevated expression throughout the healing process. Data from [63].

2.3.2.3. Metalloproteinases and Angiogenic Factors

Optimal bone healing largely depends on the establishment of an adequate blood flow within the callus as the ingrowth of blood vessels allows osteogenic precursor cells, osteoblasts and osteoclasts to invade. During the final stages of the endochondral ossification remodelling period, MMPs degrade the extracellular matrix of cartilage and bone respectively, thereby achieving the conditions required for the invasion of blood vessels. It is speculated that two classes of angiogenic factors and their receptors regulate vascularisation during fracture healing. These are the vascular endothelial growth factor (VEGF) family with the associated vascular endothelial growth factor receptors (VEGFR) and the angiopoietin family with the associated Tie receptors. VEGFs stimulate mitogenesis in vascular endothelial cells and act as a crucial mediator of neo-angiogenesis. [55,58] Unlike VEGF, angiopoietins are not mitogenic but function as a survival factor for endothelial cells by blocking apoptotic signals, stabilise cell-cell interactions of endothelial cells and stimulate the migration and spreading of endothelial cells from pre-existent vessels. [64] Thus, angiopoietins are related to the formation of collateral branches from existing vessels.

2.4. Apoptosis

Apoptosis, or programmed cell death, is an essential biological process in normal life and tissue development and is absolutely required to maintain the homeostasis and integrity of multicellular organisms. Disturbances of the balance between apoptosis and proliferation can lead to human pathologies such as cancer, degenerative conditions and atrophy. Apoptosis physiologically occurs during development. For instance, during foetal life, our fingers and toes are sculpted through apoptotic elimination of cells between developing digits. Nerve cells proliferate in excess and die when they are not able to connect to other neurons. Lymphocytes that have become auto-reactive undergo apoptosis in order to avoid autoimmune disease. Furthermore, diseased cells like virus-infected cells, tumor cells and cells with an irreparable DNA-damage are also eliminated by means of programmed cell death. [65-67]

Apoptosis must be distinguished from necrosis, which is a form of traumatic cell death leading to acute local inflammation. Necrosis occurs as a result of cellular ATP-depletion due to severe tissue damage. Affected cells undergo swelling and bursting, release their intracellular contents and consequently initiate an inflammatory response of the surrounding cells. By contrast, apoptosis is an active, ATP-requiring process which does not cause inflammation. This kind of cell death is characterised by typical morphological changes in the cell, including chromatin condensation, DNA cleavage, cell shrinkage, nuclear and cell fragmentation, and disassembly into membrane-enclosed vesicles called apoptotic bodies. [65,67,68] Phosphatidylserine, which is normally found at the inner leaflet of the plasma membrane, is translocated to the outer membrane leaflet during apoptosis. [69] This surface exposed phosphatidylserine serves as a tag for neighbouring cells or macrophages which eventually eliminate the apoptotic bodies via phagocytosis. [65,69]

A family of intracellular enzymes termed caspases (cysteine-aspartate-proteases) represent key molecules of the apoptotic process. Caspases are cysteine-containing proteases which selectively cleave specific protein substrates at the site adjacent to an aspartic acid residue. Humans have 15 different caspases [67] and all of them are synthesised as inactive proenzymes which must be cleaved in order to become an active form. Caspases can be divided into initiator caspases (e.g. caspases 8, 9, 10) which activate downstream caspases by proteolysis, and effector caspases (e.g. caspases 3 and 6) which cleave important cell components such as proteins of the nuclear lamina and cytoskeleton, resulting in the disassembly of the apoptotic cell. Furthermore, effector caspases activate a specific DNase termed CAD (caspases-activated DNase) and degrade and inactivate the DNA repair enzyme PARP (polyadenosine ribose polymerase). The activation of CADs leads to the fragmentation of genomic DNA while the inactivation of PARP inhibits repair mechanisms of damaged DNA. [65,67,68]

Figure 13 shows the different kinds of complex pathways leading to cellular apoptosis. Apoptosis can be initiated by two major pathways. The extrinsic pathway (also called the death receptor pathway) is stimulated by ligand binding to death receptors on the cell surface, whereas the intrinsic pathway (also called the

mitochondrial pathway) involves damage to different systems within the cell, such as the mitochondria, endoplasmic reticulum or nucleus. Both pathways converge at the level of caspase 3 activation, leading to the above mentioned final steps of apoptosis. [68,70]

The three major death ligands with their corresponding receptors involved in the **extrinsic pathway** are TNF-α with TNF-α receptor 1 (TNFR1), the TNF-related apoptosis-inducing ligand (TRAIL) with death receptor 4 and 5 (DR4 and DR5), and the Fas ligand with its receptor Fas (also known as CD95, member of the TNF receptor family). Ligand binding leads to the trimerisation of the death receptors and the association of the adapter protein FADD (Fas-associated death domain protein) [67,68,70], or in the case of TNF-α binding to TNFR1, the association of the adapter proteins TRADD (TNF receptor-associated death domain protein), TRAF2 (TNFR-associated factor 2), RIP1 (receptor interacting protein 1) and FADD. [71] Both the death receptors and the adapter molecules contain death domains which bind together. FADD further recruits inactive proforms of procaspase 8. This protein complex formed around the intracellular parts of the death receptor is termed death-inducing signalling complex (DISC) and aims to activate the initiator caspase 8. Once activated, caspase 8 proteolytically and directly activates the effector caspase 3 and apoptosis ensues.
Caspase 8 also cleaves the cytosolic protein Bid to a truncated active form, tBid, which then translocates to mitochondria, inducing cytochrome c release through the activation of Bak or Bax (see below). Normally cytochrome c is bound to the outer surface of the inner membrane of the mitochondrion and is an important component of the mitochondrial electron transfer chain. Once released into the cytosol, it binds to Apaf-1 (apoptotic protease activating factor-1). Apaf-1 exists in the cytosol as an inactive monomer bound to dATP. The interaction with released cytochrome c leads to hydrolysis of the bound dATP to dADP, to a change in the conformation of Apaf-1 and finally to the assembly of Apaf-1 and procaspase 9 into a haptomeric complex termed apoptosome. The apoptosome activates the initiator caspase 9, which in turn activates the effector caspase 3. [67,68,70]

The **intrinsic pathway**, which is either initiated by mitochondrial or endoplasmic reticulum stress or by irreparable DNA damage, leads to mitochondrial cytochrome

c release causing the same events as above described. This cytochrome c release is regulated by complex interactions of the Bcl-2 family proteins at the surface of the mitochondria. Members of the Bcl-2 family are single-pass transmembrane proteins which either enhance the release of mitochondrial proteins such as cytochrome c, or alternatively inhibit it. So Bcl-2 family members can be divided into proapoptotic proteins like Bax, Bak, Bad, Bid, Bim, Puma, Noxa and antiapoptotic proteins like Bcl-2 (it was first discovered in a follicular B cell lymphoma, leading to the name Bcl) and Bcl-xL. After their activation through various death-inducing stimuli like Bim and Bid, Bax and Bak induce cytochrome c release. The activation of Bax and Bak involves the translocation of Bax monomers from the cytosol to the outer mitochondrial membrane (Bak is constitutively mitochondrial), the conformational change of Bax and Bak, and finally the oligomerisation of the monomers to homodimeric molecules. Oligomeric Bax and Bak are capable of forming channels in the mitochondrial membrane that induce mitochondrial outer membrane permeabilisation resulting in cytochrome c release. Bcl-2 inhibits Bax and Bak through the formation of inhibitory heterodimeric complexes with Bax and Bak and therefore avoids cytochrome c release. Conversely, Puma, Noxa and Bad inhibit the function of antiapoptotic Bcl-2 proteins. [67,68,70]

DNA damage, for instance caused by ultraviolet or gamma irradiation, leads to the activation of the transcription factor p53 which enhances the expression of genes for apoptosis or cell-cycle arrest, especially the proapoptotic proteins Puma, Noxa, and Bax for apoptosis, and p21 for cell cycle arrest. [68]

Mitochondrial stress, for example due to ischemia, Ca^{2+} overload or exposure to reactive oxygen species, causes cytochrome c release and the activation of the downstream caspase cascade as above mentioned. Moreover, endoplasmic reticulum stress inhibits ER calcium pumps, leading to Ca^{2+} release into the cytosol, which in turn results in mitochondrial cytochrome c release. ER calcium release also activates phospholipase A2 and the formation of arachidonic acid, another promoter of cytochrome c release. Additionally, ER calcium depletion perturbs the proper folding of newly formed proteins and so causes the formation of unfolded and misfolded proteins. The endoplasmic reticulum possesses several sensors of ER stress such as Ire1 and ATF6 which are activated by un-/misfolded proteins. Initially, Ire1 and ATF6 stimulate the expression of proteins that can

increase the protein-folding capacity of the ER. If un-/misfolded proteins persist, Ire1 and ATF6 support the expression of the protein CHOP. Moreover, Ire-1 associates with the adapter molecule TRAF2 to activate caspase 12 and the kinase JNK. Caspase 12 then activates caspase 3, whereas JNK together with CHOP causes mitochondrial cytochrome c release. [68]

In addition to Bcl-2, inhibitors of apoptosis proteins (IAPs) are another factor in the suppression of apoptosis by means of their direct inhibition of caspases. However, the activity of IAPs is suppressed or cleaved by the proteins Smac/Diablo and HtrA2/Omi which are released from mitochondria together with cytochrome c during apoptosis signalling. Two other mitochondria-associated proteins are released together with cytochrome c: apoptosis-inducing factor (AIF) and endonuclease G. Both promote chromatin condensation and DNA degradation. [67,68]

Another survival pathway involves NFκB signalling. TNF-α binding to TNFR1 induces the association of the kinase IKK to the adapter molecule TRAF2. Activated IKK phosphorylates IκB, the endogenous inhibitor of NFκB, which in turn releases NFκB and so relieves the inhibition of NFκB, allowing the molecule to translocate to the nucleus and activate the expression of survival factors including IAPs and proapoptotic Bcl-2 family members. [68,71]

Apoptosis can also be initiated by the withdrawal of growth factors. When growth factors, promoting cell survival, bind to their corresponding receptors, PI-3 kinase activity is stimulated, leading to the downstream activation of protein kinase B (PKB, also known as Akt). One result is the phosphorylation and inactivation of the proapoptotic protein Bad, which in turn is no longer able to inhibit the antiapoptotic Bcl-2 proteins. In case of a withdrawal of growth factors, Bad remains unphosphorylated and active, thus suppressing antiapoptotic Bcl-2 proteins, resulting in cytochrome c release. [65,67,68]

To summarise, the induction or inhibition of the apoptotic pathway is under the control of highly complex molecular events and is dependent on the relation between proapoptotic factors and antiapoptotic factors.

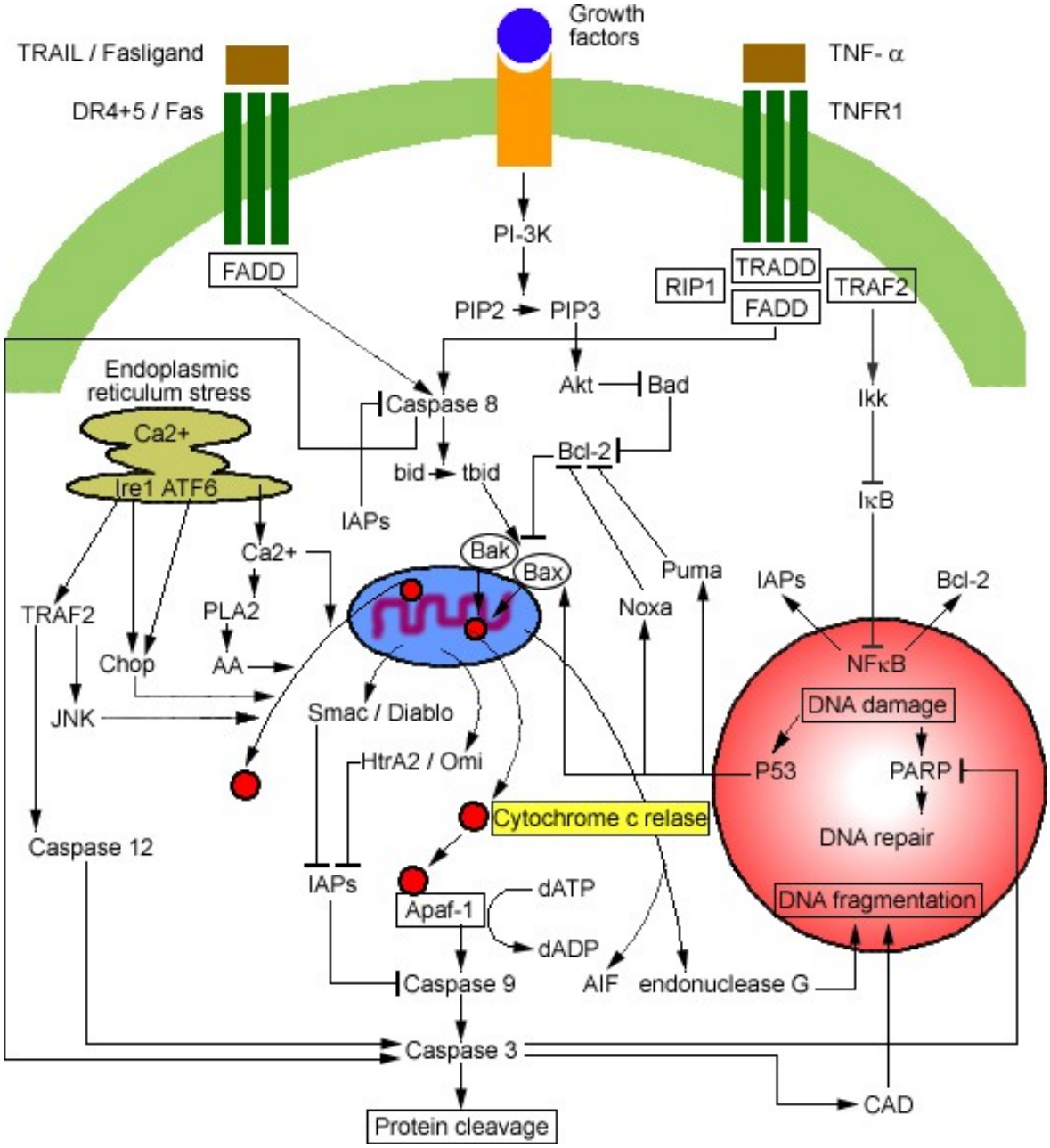

Figure 13: Schematic representation of apoptotic signalling from the plasma membrane, mitochondrium (blue), nucleus (red) and endoplasmic reticulum. For details see text.

2.4.1. Tools for the Study of Apoptosis

A variety of techniques (e.g. flow cytometry, immunofluorescence microscopy, light microscopy, ELISA, gel electrophoresis, or Western blots) are currently available for the detection and measurement of apoptotic cells. Different assays can be

used to study various apoptotic stages or targets. Examples of apoptotic-studying methods are:

- measurement of caspase activity
- Annexin V labelling for the detection of phosphatidylserine externalisation occurring as a result of membrane alterations
- qualitative or quantitative measurement of DNA fragmentation (by means of gel electrophoresis, ELISA or TUNEL)
- measurement of the expression of apoptosis-related proteins such as Fas, PARP, p53, Bcl-2, Bax and Bad
- detection of caspase-cleavage epitopes in cytokeratin 18
- measurement of mitochondrial membrane potential
- evaluation of ultrastructural morphological cell changes by electron microscopy

The decision to use a specific tool depends on the stage and apoptotic alteration one wants to detect, but also on the type of cells one intends to study (e.g. cell populations or single cells, cell cultures, blood cells or tissue sections). [69,72,73]

There is much literature on the success and specifity of TUNEL (**t**erminal deoxynucleotidyl transferase (TdT)-mediated d**U**TP **n**ick **e**nd **l**abelling) staining and also on the functioning of this assay when performed on epiphyseal cartilage of bone [74-78]. This method allows the sensitive identification of single apoptotic cells at a very early stage of apoptosis; additionally the tissue architecture and histology can be evaluated. [74]

DNA fragmentation into mono- and oligonucleosomal fragments and single strand breaks by endogenous endonucleases like CAD typifies apoptosis. [79] This process takes place very early during apoptosis. DNA fragmentation is the most characteristic biochemical event during apoptosis, referred to as the hallmark of programmed cell death. [74,78] The single strand breaks (so called “nicks”) can be detected by labelling their free 3’-OH termini with modified nucleotides in an enzymatic reaction that is catalysed by the enzyme terminal deoxynucleotidyl transferase (TdT).

3. MATERIALS AND METHODS

A rat model was used to examine the apoptosis rate of chondrocytes at the growth plate after fracture of long bones. All animal experiments were approved by the Austrian Federal Ministry of Science and Research (file number: BMBWK-66.010/0054-BrGT/2006).

The task of analysing physeal chondrocytes undergoing apoptosis was accomplished using an immunohistochemical staining called TUNEL assay.

The animal experiments, the ensuing tissue preparation, as well as the immunohistochemical procedure were performed at the special laboratories of the Center for Medical Research of the Medical University of Graz.

3.1. Materials

The following tables declare all used materials and devices.

Table 1: Animals and pharmaceuticals

Label	Particulars	Manufacturer
Sprague-Dawley rat	56 male rats	Medical University Vienna, 2325 Himberg
Forane®	Isoflurane, volatile anaesthetic, 100 ml	Abbott Laboratories
Hydrogen chloride	HCl 37%, 50 ml	Merck KGaA
Ketanest-S®	2 ml, 25 mg/ml	Pfizer Corporation Austria GesmbH
Novalgin® drops	Metamizole, 10 ml solution	Sanofi-aventis GmbH
Physiological saline solution	Solution for infusion, 50 ml	Fresenius Kabi Austria GmbH
Rimadyl®	Carprofen, 20 ml solution	Pfizer Corporation Austria GesmbH
Rompun®	Xylazine	Pfizer Corporation Austria GesmbH
Thiopental Sandoz®	Thiopental 1 g	Sandoz GmbH

Table 2: Chemicals

Label	Particulars	Manufacturer
Acetone*	For analysis	Merck KGaA
DAB	Liquid DAB substrate, chromogen system	DakoCytomation
Ethanol*	Absolute, for analysis	Merck KGaA
Ethylenediamine tetraacetic acid disodium salt dihydrate	Reagent grade, ~99%	Sigma-Aldrich Co.
Formaldehyde solution	10%	Donauchem HandelsgmbH
GLC™ Mounting Medium*	Xylene-based, low viscosity mounting medium	Sakura Finetek Europe B.V.
Hydrogen peroxide	30%	Merck KGaA
In Situ Cell Death Detection Kit, POD	1 TUNEL kit (50 tests)	Roche Diagnostics GmbH
Mayer's hemalum*	pH 2.26	Gatt-Koller GmbH
Methanol*	GR for analysis	Merck KGaA
PBS*	pH 7.2-7.3, 10 000 ml containing reagents: sodium chloride, disodium hydrogen phosphate, potassium dihydrogen phosphate	Pharmacy of the Medical University Graz Single reagents by Merck KGaA
Proteinase K	Recombinant, PCR Grade; lyophilizate	Roche Diagnostics GmbH
Sodium hydroxide	Pellets GR for analysis	Merck KGaA
Xylene*	Isomers, >98%, pure, for histology	Carl Roth GmbH + Co. KG

* Products were kindly provided by the Center for Medical Research of the Medical University of Graz.

Table 3: Laboratory instruments and consumables

Product name	Particulars	Manufacturer
Coverglasses*	20 x 20 mm	Carl Roth GmbH + Co. KG
Dako Pen	Delimiting pen	DakoCytomation
Embedding cassettes*	Universal, white	Sanowa Laborprodukte GmbH
Micro Slides	X-tra™ adhesive, precleaned, white, 26 x 76 x 1.0 mm	Surgipath Europe Limited
Microcentrifuge tubes	1500 µl	Eppendorf AG
Pipette tips	epTIPS-pipette tips	Eppendorf AG
Pipettes*	Research Series 2100 adjustable, single channel	Eppendorf AG
Rotilabo® round filters*	Filter paper for qualitative analysis, 240 mmm	Carl Roth GmbH + Co. KG
Vogel Histo-Comp®*	Paraffin wax, melting point 56°C	Vogel GmbH & Co. KG

* Products were kindly provided by the Center for Medical Research of the Medical University of Graz.

Table 4: Laboratory equipment

Device	Type and description	Manufacturer
Cooling plate	COP 30 For rapid cooling of paraffin blocks during tissue processing or cutting; -20°C – +15°C	Medite GmbH
Microbiological incubator	BD 115, BD 53, BD 240	Binder GmbH
Microscope	Olympus BX53, universal; upright inspection and research microscope	Olympus Corporation
Precision balance	Sartorius CP225D-OCE	Sartorius AG
Rotary microtome	Microm HM 360 Electronic motorised microtome	Microm Micromarketing-Systeme und Consult GmbH

Scan Scope	ScanScope T3 Scanner for creating digital slide images	Aperio Technologies, Ltd.
Tissue embedding console system	Tissue-Tek® TEC™	Sakura Finetek Europe B.V.
Vortex	TTS 2	IKA Labortechnik GmbH & Co. KG
Water purification system	Milli-Q Gradient A10 For the production of Type II analytical-grade water	Millipore Corporation

All devices mentioned in Table 4 are part of the infrastructure of the Center for Medical Research.

3.2. Animal Experiments and Protocols

Fifty-six male Sprague-Dawley rats aged 4 weeks and weighing 100 to 120 grams were purchased from the Division for Laboratory Animal Science and Genetics in Himberg (Medical University Vienna, Core Unit for Biomedical Research). During the experimental period, the animals were housed in the special animal laboratory of the Center for Medical Research of the Medical University of Graz. They were caged in pairs with a light to dark cycle of 12:12 and received special forage for mice and rats, purchased from the Institute for Biomedical Research (Medical University Graz, 8036 Graz), and purified water charged with hydrogen chloride 37% (8.6 ml HCl per 20 l water).

The rats were randomly distributed into two main groups, the experimental and the control group, which were further divided into several subgroups, depending on the day of post-fractural euthanasia. Each subgroup consisted of seven rodents (Table 5).

Figure 14: Sprague-Dawley rats in their litters.

Table 5: Animal allocation into groups

Main group	Subgroup	Number of Rats	Procedure	Day of Euthanasia
Experimental Group	1	7	fracture on day zero	day 3
	2	7	fracture on day zero	day 10
	3	7	fracture on day zero	day 14
	4	7	fracture on day zero	day 29
Control Group	1	7	no fracture	day 3
	2	7	no fracture	day 10
	3	7	no fracture	day 14
	4	7	no fracture	day 29

3.2.1. The Fracture

The rodents of the experimental group were subjected to a transverse middiaphyseal fracture of the left tibia. Therefore, on day zero they were moved to the operating room where surgery was performed. After weighing the rat, anaesthesia was performed by an intramuscular injection of Ketanest-S® 90 mg/kg body weight and Rompun® 5 mg/kg body weight. A guillotine was applied in order to induce a closed transverse middiaphyseal fracture. Thereby a piece of iron weighing 500 g was dropped from the height of 20 cm to cause a closed diaphyseal fracture of the rat's left tibia. For protocol, the weight of the animals as well as the starting and ending time of anaesthesia were documented.

Postoperatively, rats were returned to their litters for nursing and activity ad libitum. Painkillers (Rimadyl® 4-5 mg/kg body weight) were injected subcutaneously every 24 hours to ensure analgesia. After seven days Rimadyl® was discontinued and subsequently Novalgin® drops (20 gtt per 400 ml) were added to the drinking water. Simultaneously, the control animals also received painkillers in order to ensure that the members of both groups only differed according to whether fracture had taken place or not.

3.2.2. Euthanasia

Depending on the subgroup, euthanasia was performed 3, 10, 14 and 29 days after fracture. The control rodents were sacrificed on the same days as experimental animals; it was therefore possible to compare the age and the weight between the animals of both main groups.
For killing, the animals were narcotised with volatile anaesthetic Forane® and then sacrified by an intracardial Thiopental Sandoz® injection. Posthumously, the rats were weighed again. Subsequently, the left and right tibiae were harvested and cautiously dissected from soft tissue. An extension of the fracture callus into the growth plate never occurred.

Figure 15: Unfractured right tibia of a rat weighing 165 g.

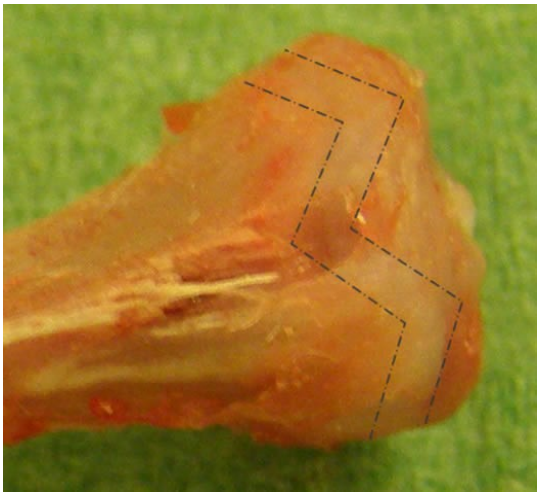

Figure 16: Tibia with marked growth plate.

3.3. The Treatment of the Bones

The removed and prepared bones were fixed in formaldehyde solution 10% for up to 24 hours before undergoing decalcification in EDTA pH 7.0.

For the production of this particular EDTA solution, 125 g ethylenediamine tetraacetic acid disodium salt dehydrate, 13 g sodium hydroxide pellets and 875 ml distilled water were mixed well until the liquid appeared clear.

The chelating agent EDTA had to be changed every 24 hours; this procedure lasted for 2 weeks. Afterwards, the decalcified bones were dehydrated in ethanol 70% at 60°C for 2 hours, then in ethanol 96% at 60°C for 4 hours and eventually in acetone at 60% for 1 hour. Finally, the tissue was incubated in liquid paraffin for 1 hour.
The embedding machine Tissue-Tek TEC was used for embedding the bones in paraffin in order to make them preservable and accessible for cutting.

3.4. TUNEL Assay

Apoptotic cells were visualised using **t**erminal deoxynucleotidyl transferase (TdT)-mediated d**U**TP **n**ick **e**nd **l**abelling (TUNEL). Gavrieli and collaborators established this method as a specific, simple and reproducible tool for the in situ detection and quantification of programmed cell death at a single-cell level whilst also preserving tissue architecture and enabling the additional visualisation of apoptotic morphological changes. [74] TUNEL is based on labelling DNA strand breaks, which can be found at a very early stage of programmed cell death and are the hallmark of apoptosis, using terminal deoxynucleotidyl transferase (TdT) to incorporate labelled nucleotides. Several researchers have successfully applied this TUNEL method to the tibial or femoral growth plates of rats. [75-77]

In order to perform the TUNEL assay, the *In Situ Cell Death Detection Kit, POD* from Roche Diagnostics was utilised. Left and right tibiae of the experimental animals and left tibiae of the control animals were used for TUNEL staining.

This TUNEL assay comprises three main stages. Firstly, DNA strand breaks are labelled with fluorescein-labelled nucleotides. The enzyme terminal deoxynucleotidyl transferase (TdT) catalyses the polymerisation of labelled nucleotides to free 3'-OH DNA ends. Secondly, incorporated fluorescein is detected by anti-fluorescein sheep antibody fragments, which are conjugated with horse-radish peroxidase (POD). Finally, substrate for POD such as diaminobenzidine (DAB) is added to make stained cells accessible for visualisation under light microscope.

3.4.1. Tissue Preparation

The tibial paraffinblock samples were clamped into the rotation microtome HM360 in order to cut tissue sections at 4 µm. Trimming had to be undertaken incredibly carefully so that sections would contain the entire epiphyseal plate of the tibia. Nevertheless, in some cases it was not possible to avoid partial physeal dissociation from the metaphyseal portion of the bone.

Tissue sections were mounted on coated slides (Micro Slides x-tra™ adhesive by Surgipath) to enhance tissue adherence. These special microscope slides have a permanently positively charged surface, which helps to bond tissue sections without the use of additional adhesives.

Slides were stored at 37°C for at least 10 hours in order to become dry and incubated at 60°C for 1 hour in order to melt the paraffin coat before proceeding with deparaffinisation. For this purpose, slides were immersed in xylene for 5 minutes and a second time in new xylene for 10 minutes. Hydration was completed by transferring the slides in a descending ethanol series; more precisely in absolute ethanol, 90% ethanol, 70% ethanol and 50% ethanol twice for 3 minutes each. Rehydrated sections were rinsed in PBS twice for 5 minutes each.

A total of 10 slides could be processed during each staining run. Two tissue sections were affixed to one object holder, enabling the treatment of 18 tibial tissue slices as well as one positive and one negative control for each staining run (Figure 17).

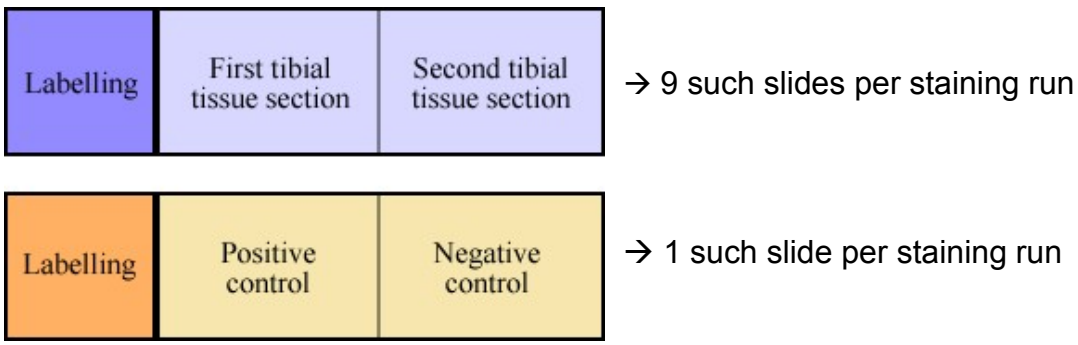

Figure 17: Arrangement of tissue sections on microscope slides

3.4.2. Proteinase K

For permeabilisation, tissue sections had to be incubated with proteinase K, 20 µg/ml, for 15 minutes at room temperature.
Firstly, 10 mg (weighed using a precision balance) of lyophilised proteinase K were mixed with 1 ml PBS, then separated into 5 aliquots of 200 µl and frozen for stocking. When needed, one aliquot of such prepared proteinase K was warmed up at room temperature and added to 100 ml distilled water, resulting in the required concentration of 20 µg/ml.
The treatment with proteinase K 20 µg/ml for 25 minutes was followed by soaking the slides in PBS twice for 4 minutes each.

3.4.3. Hydrogen Peroxide

Endogenous peroxidase activity was blocked with 3% hydrogen peroxide in PBS at room temperature. Therefore 90 ml of PBS and 10 ml of 30% hydrogen peroxide were poured into a glass jar. Slides were submerged in this solution for up to 30 minutes and afterwards washed twice in PBS.

3.4.4. TUNEL Reaction

The *In Situ Cell Death Detection Kit, POD* from Roche Diagnostics consists of the following reagents:

1. Enzyme Solution
   - Terminal deoxynucleotidyl transferase from calf thymus, recombinant in E. coli, in storage buffer
   - 10x concentration
   - 5 x 50 µl
2. Label Solution
   - Nucleotide mixture in reaction buffer
   - 1x concentration
   - 5 x 550 µl
3. Converter-POD
   - Anti-fluorescein antibody, Fab fragment from sheep, conjugated with horse-radish peroxidase (POD)
   - Ready-to-use
   - 3.5 ml

Immediately before use, the TUNEL reaction mixture was prepared. The total volume (50 µl) of one vial Enzyme Solution was added to 450 µl Label Solution to obtain 500 µl TUNEL reaction mixture, which was mixed well with a vortex mixer in order to equilibrate the components. For one staining run, a total amount of 950 µl TUNEL reaction mixture was required.

The area around the tissue sections was dried and each histological slice was surrounded with a delimiting pen to create a hydrophobic demarcation which would avoid the outflow of the reagents. Each sample was covered with 50 µl TUNEL reaction mixture, except for the negative control, which was covered with 50 µl Label Solution (without terminal transferase). Slides were placed in a humidity chamber to decrease reagent evaporation and were incubated at 37°C for 1 hour. During incubation time, the so called TUNEL-reaction proceeded, showing that the terminal transferase catalyses the polymerisation of labelled deoxynucleotides to free 3'-OH DNA ends in a template-independent manner. After 60 minutes the reaction was terminated by washing the slides with the washing buffer PBS two times.

3.4.5. Signal Conversion

The fluorescein-labelled nucleotides can be detected by the use of anti-fluorescein antibody conjugated with POD. The area around the samples was dried and sections were covered with 50 µl Converter-POD (supplied with the TUNEL kit). Slides were incubated in a humidity chamber at 37°C for 30 minutes before being rinsed twice with PBS.

Diaminobenzidine was used to produce a dark brown precipitate in the presence of POD and thus to highlight nuclei with DNA fragmentation. 50 µl DAB were applied directly onto tissue sections and left thereon at room temperature for about 1 minute. Reaction had to be followed under a light microscope in order to ascertain the exact time required to wash out the substrate in PBS.

The treated sections were counterstained with filtrated Mayer's hemalaun solution for 10 seconds then rinsed well with warm running tap water for 2 minutes. After

dehydration in 50%, 70% and absolute ethanol for 1 minute each and cleaning in xylene twice for 2 minutes, tissue sections were coverslipped with GCL™ mounting medium and left for evaluation with an optical microscope.

3.4.6. Control Sections

The accuracy of the TUNEL method was evaluated using control specimens. Positive controls were obtained on sections of rat small intestine, submitted to the same treatment as tibial tissue sections. In addition, bone marrow cells were used as an internal positive control. In negative control sections, the enzyme TdT was omitted from the reaction mixture.

3.5. Digital Slide Images

For further tissue analysis, TUNEL-stained tissue sections were scanned with Aperio's ScanScope scanner, used to create digital slide images. These digital images with the file format *svs* were converted and compressed into a *jpeg*-format by means of the module Digital Slide Studio, which is included in the Aperio Digital Slide Information Management Software. The *jpeg*-images could then be opened with the ImageJ Software, a Java-based image processing program.

3.6. Quantification of Apoptotic Cells

TUNEL-positive cells of the proximal tibial growth plate were counted manually using ImageJ Cell Counter. Unfortunately, the digital image quality was suboptimal for the accurate differentiation of apoptotic (meaning TUNEL-positive) and non-apoptotic cells. Thus, each nucleus had to be additionally evaluated with an optical microscope under 60-fold magnification.

Cells were considered as TUNEL-positive where the following criteria were met:

- Colour: brown, dark brown or black nucleus
- Morphology: nuclear staining has a crescent, annular, or fragmented shape, or alternatively the whole nucleus is stained

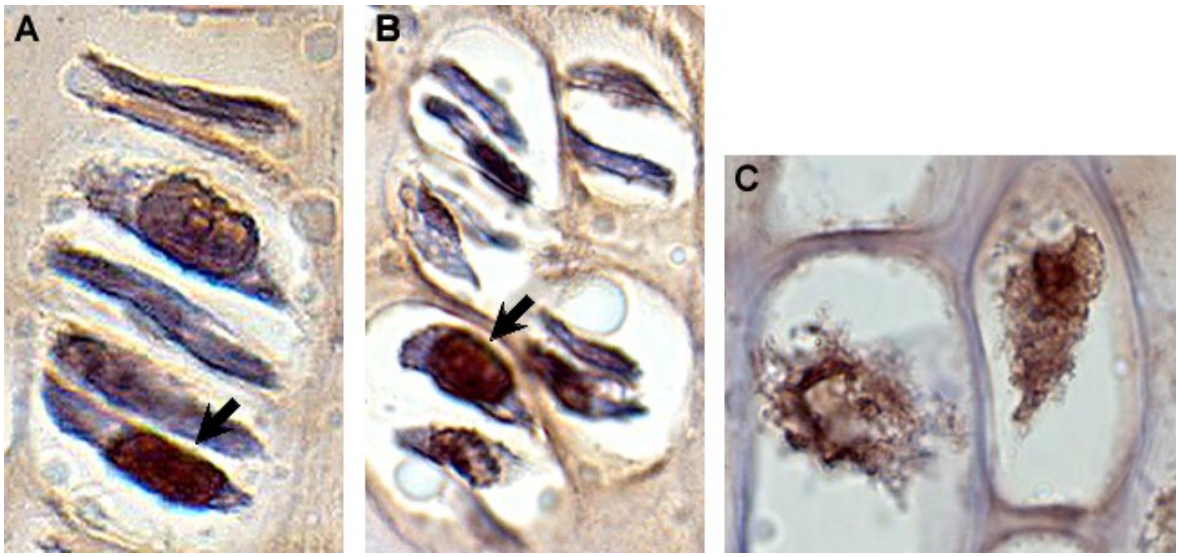

Figure 18: TUNEL-positive chondrocytes. *(A and B)* Arrows show apoptotic brown-coloured cell nuclei in the columnar zone of the tibial growth plate. In non-apoptotic cells the nucleus is dyed a bluish colour. *(C)* Apoptotic nuclei of hypertrophic chondrocytes become condensed and fragmented. TUNEL staining. Light microscopy. Original magnification x60.

According to Gavrieli and co-workers, DNA fragmentation in apoptotic cells is initiated at the nuclear periphery and progresses towards the centre. Consequently, the TUNEL-staining pattern in apoptotic nuclei changes over time, starting with a crescent shape in cells just entering programmed cell death, followed by an annular pattern and finally leading to the staining of the whole nucleus. In its final stage the nucleus becomes condensed and fragmented. [74]

3.6.1. Partition of the Growth Plate into Different Regions and Zones

The growth plate of a tissue section was split into 3 different regions:

- lateral I
- central
- lateral II

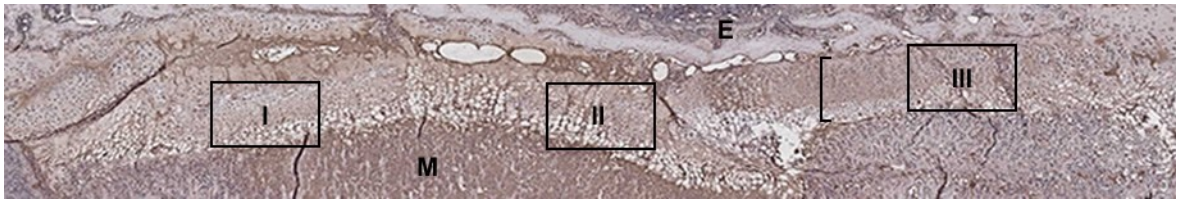

Figure 19: Tibial growth plate - division into 3 regions. *(I)* lateral I region, *(II)* central region, *(III)* lateral II region. The bracket marks the full length of the epiphyseal plate, which is located between the epiphysis *(E)* and the metaphysis *(M)*. TUNEL staining. Light microscopy.

Each of these regions was further subdivided into 2 zones:

- columnar zone
- hypertrophic zone

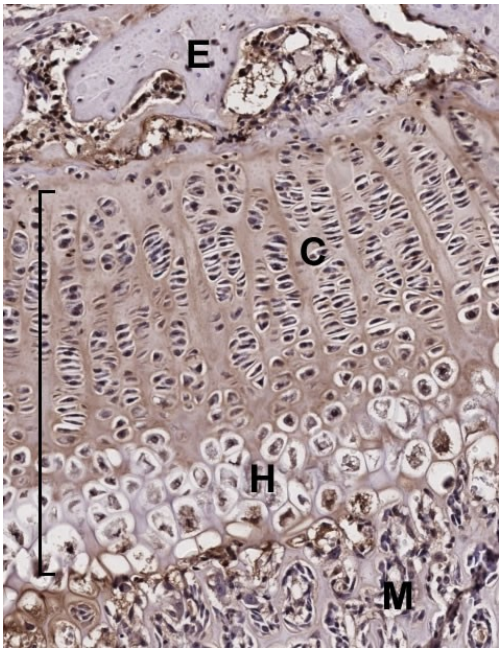

Figure 20: Tibial growth plate - division into 2 zones. *(C)* columnar zone, *(H)* hypertrophic zone. The bracket marks the full length of the growth plate, which separates the epiphysis *(E)* and the metaphysis *(M)*. TUNEL staining. Light microscopy.

This separation resulted in 6 different areas:

- **lateral I – columnar zone**
- **lateral I – hypertrophic zone**
- **central – columnar zone**
- **central – hypertrophic zone**
- **lateral II – columnar zone**
- **lateral II – hypertrophic zone**

The frequency of apoptotic physeal chondrocytes was measured in all of the above 6 areas. In each area 100 cells, regardless of colour and morphology, were manually and arbitrarily enumerated. Out of these 100 cells, TUNEL-positive cells were counted. This number was then defined as the apoptosis rate.

Apoptosis rate [%] = number of apoptotic chondrocytes / 100 cells

The apoptosis rates of the 3 different regions (lateral I, central, lateral II) were finally averaged; hence, the mean apoptosis rate of the hypertrophic zone, the columnar zone and the entire growth plate was obtained.

3.7. Statistical Analyses

Statistical analyses were performed with the assistance of Mag.rer.nat. Andrea Groselj-Strele from the Office for Biostatistics of the Center for Medical Research of the Medical University of Graz. SPSS version 15.0.1 (SPSS Inc., Chicago, Illinois, USA) was used for statistical data analysis and data presentation.

All data are presented as median (p25 - p75 percentiles). Normality of data was checked using the Shapiro-Wilks test.

Mann-Whitney *U* tests were used for 2-group comparison (experimental group versus control group) because of non-normal distributed data.
The Wilcoxon signed-rank test was performed to evaluate the discrepancy in the rate of apoptosis between the fractured and the contra-lateral intact bone of the experimental animal.

A potential disparity in the apoptosis percentage between the four subgroups (group day 3, day 10, day 14 and day 29) within the experimental group and the control group, respectively, was tested using the Kruskal-Wallis test with subsequently performed pairwise comparisons with Bonferroni corrections. Additionally, the Friedman test was carried out for confirmation.

The difference in the apoptosis rate between the hypertrophic zone and the columnar zone of the epiphyseal plate in one animal was evaluated using the Wilcoxon signed-rank test.

A p-value of less than 0.05 was considered as statistically significant.

4. RESULTS

4.1. Fractured Bone versus Contra-lateral Bone

The percentages of apoptotic cells within the growth plates of the fractured and the contra-lateral bones of the experimental group are shown in Table 6. As seen in Figure 21, the epiphyseal plate of the left fractured tibia showed a higher physeal apoptosis rate compared to the contra-lateral intact tibia. This was found to be statistically significant on all evaluated days.

The apoptosis rate of the fractured tibia rose continuously over time, however, without statistical significance. The maximum level of physeal apoptotic cells could be observed on day 29 (Figure 21). The trend of a continuous increase of the apoptosis incidence over time could be described neither for the contra-lateral intact bone of the experimental group, nor for the control bone. The apoptosis percentage of both intact tibiae consisted more of an irregular rising and falling over time, without a significant difference in the apoptosis rate between singular days, with only one exception: the control bone showed a significant increase in chondrocyte apoptosis from day 14 to day 29. This is valid for the columnar zone ($p = 0.006$), the hypertrophic zone ($p = 0.002$) and the entire growth plate ($p = 0.003$). The indicated p-values were calculated with the Kruskal-Wallis test with subsequently performed pairwise comparisons with Bonferroni corrections.

Table 6: Summary of the physeal apoptosis rates (in %) of the left and right tibiae of the experimental group. The median, the first and third quartile (in parentheses), and the p-value are documented. The Wilcoxon test was used. * $p < 0.05$

	Experimental group		
	Left tibia (fractured)	**Right tibia (unfractured)**	**p-value**
Day 3	21.00 (16.00 – 25.17)	14.33 (13.33 – 19.83)	**0.018***
Day 10	22.00 (16.33 – 27.50)	16.50 (12.83 – 19.33)	**0.043***
Day 14	22.17 (19.83 – 24.50)	16.50 (15.50 – 19.00)	**0.018***
Day 29	25.00 (21.83 – 26.17)	15.33 (15.17 – 18.50)	**0.018***

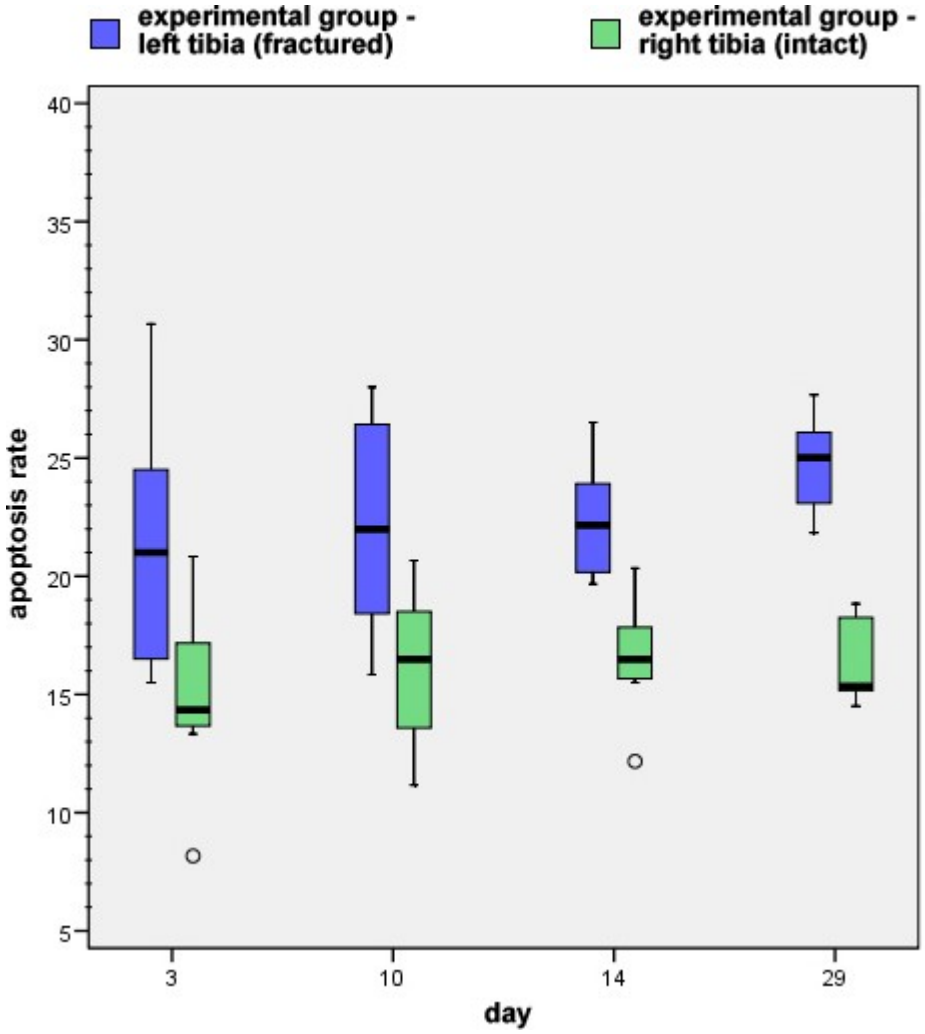

Figure 21: The apoptosis percentages of the fractured left (blue) and unfractured right (green) tibiae of the experimental group are shown in graph (n = 7, each). The X-axis represents the number of days post-traumatic on which euthanasia was carried out on the rats. The Y-axis specifies the apoptosis rate in %. The lines within the boxes indicate the median (50th percentile), the upper and lower ends of the boxes indicate the first quartile (25th percentile) and the third quartile (75th percentile), respectively. Significance ($p < 0.05$) was reached on all days.

4.2. Fractured Bone versus Control Bone

With regards to the percentage of apoptosis, an evaluation of the difference between the growth plate of the left tibia of the experimental group and the left tibia of the control group revealed a significantly higher apoptosis rate in the fractured bone on day 10, 14 and 29, but not on day 3 (Figure 22). Table 7 shows

the incidence of apoptosis for both groups and statistically important differences between them.

When separately examining the apoptosis rate of the columnar and hypertrophic zones, the columnar zone of the left fractured tibia showed significantly higher ($p < 0.01$) apoptosis percentages compared to the columnar zone of the control bone from day 10 onwards. Instead, this significance was only reached on day 14 for the hypertrophic zone. This leads to the assumption that the overall increase of apoptotic cells in the fractured bone is primarily driven by the rise of apoptosis in the columnar zone. (Figure 23)

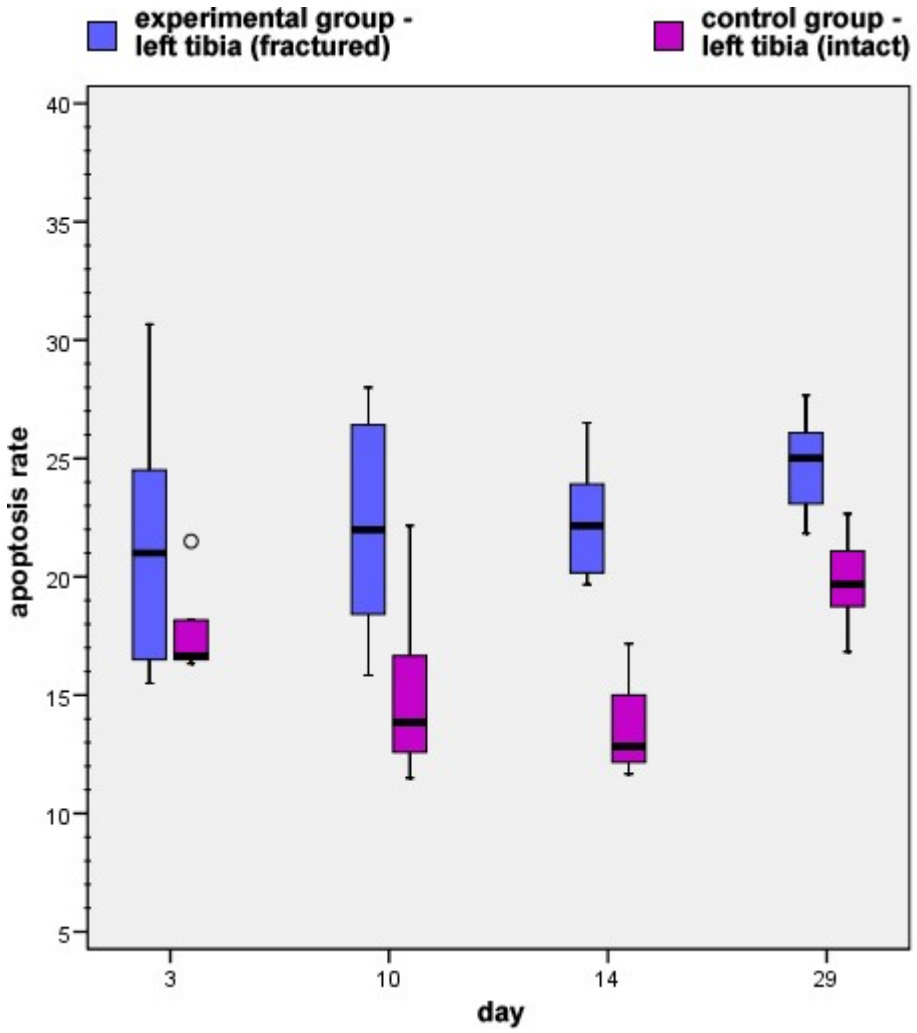

Figure 22: The apoptosis rates (in %) of the fractured left tibia of the experimental group (blue) and of the left tibia of the control group (violet) are shown in graph (n = 7, each). Significance could be reached on day 10 ($p < 0.05$), day 14 and day 29 (both $p < 0.01$).

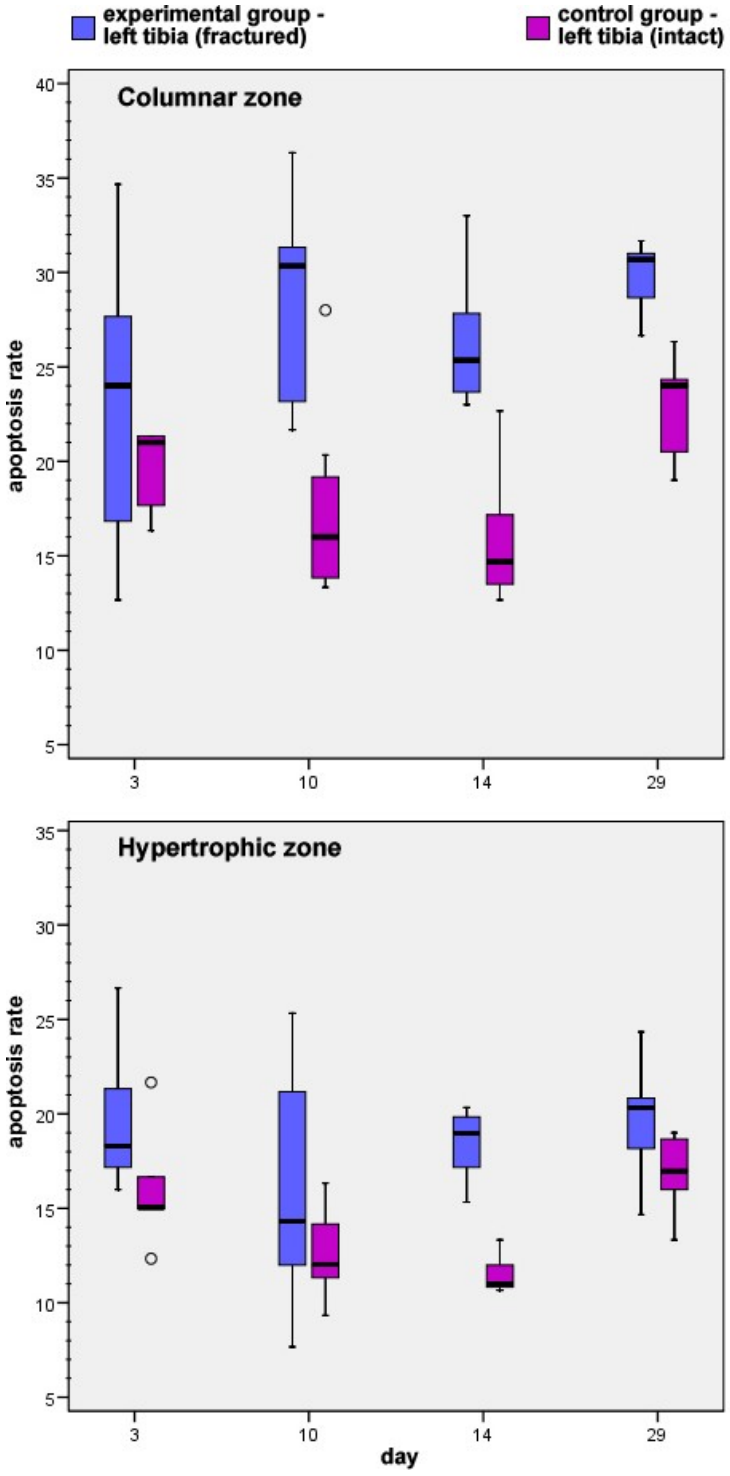

Figure 23: The apoptosis rates (in %) of the fractured left tibia of the experimental group (blue) and of the left tibia of the control group (violet) were analysed separately for the columnar zone (upper figure) and the hypertrophic zone (lower figure) of the growth plate. With regards to the columnar zone, significance could be reached on day 10 (p-value 0.006), day 14 (p-value 0.002) and day 29 (p-value 0.004), whereas the apoptosis rates of the two hypertrophic zones (those of the fractured bone and of the control bone) only showed a significant difference on day 14 (p-value 0.002).

Table 7: Summary of the physeal apoptosis rates (in %) of the left tibia of the experimental group and of the left tibia of the control group. The median, the first and third quartile (in parentheses), and the p-value are documented. The Mann-Whitney *U* test was used.
* $p < 0.05$; ** $p < 0.01$

	Experimental group Left tibia (fractured)	Control group Left tibia (unfractured)	p-value
Day 3	21.00 (16.00 – 25.17)	21.00 (17.00 – 21.33)	0.465
Day 10	22.00 (16.33 – 27.50)	16.00 (13.67 – 20.33)	**0.018***
Day 14	22.17 (19.83 – 24.50)	14.67 (13.00 – 17.67)	**0.002****
Day 29	25.00 (21.83 – 26.17)	24.00 (20.33 – 24.67)	**0.004****

4.3. Contra-lateral Bone versus Control Bone

The right intact tibia of the experimental group never demonstrated a significantly higher physeal apoptosis rate compared to the unfractured left tibia of the control group. There was no significant difference in the incidence of apoptotic death between both intact bones on day 3 (p-value 0.123), day 10 (p-value 0.522) and day 14 (p-value 0.055). However, day 29 revealed an unexpectedly and significantly higher apoptosis rate of the control bone (p-value 0.010). (Figure 24)

4.4. Columnar Zone versus Hypertrophic Zone

The amount of apoptotic cell bodies was constantly higher in the columnar zone of the growth plate than in the hypertrophic zone, regardless of which group the bone belonged to. The hypertrophic zone contained many empty lacunae of degenerated hypertrophic chondrocytes as well as lacunae with only debris or extracellular matrix (Figure 25). Such lacunae which were devoid of nuclei were not counted as apoptotic cell bodies as only those cells with a visible black or brown apoptotic nucleus were considered as TUNEL-positive.

Generally, apoptosis was spread uniformly over the full physeal width. Increased apoptosis in a more lateral or central region was not observed.

Positive controls showed staining as expected and negative controls lacked any TUNEL-positive cell. (Figure 26)

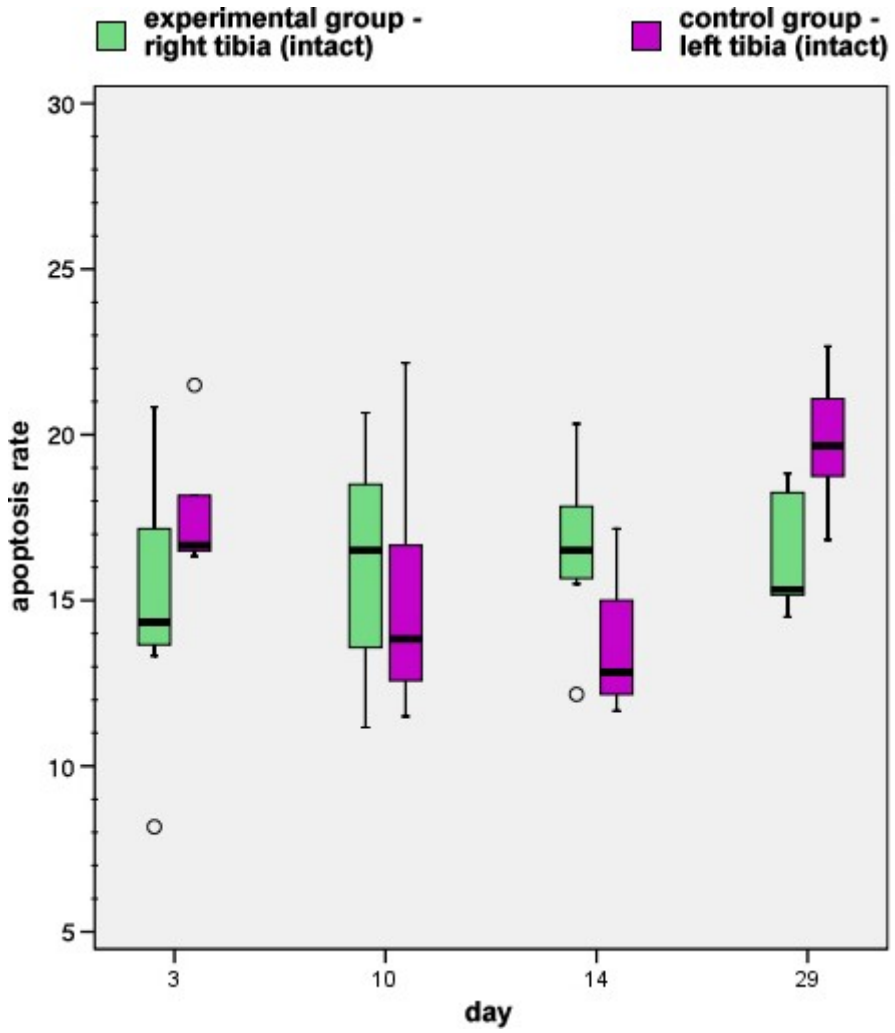

Figure 24: Physeal apoptosis rates (in %) of the right intact tibia of the experimental group compared to the left intact tibia of the control group. (n = 7, each). No significant differences were noted, except on day 29 (p = 0.01).

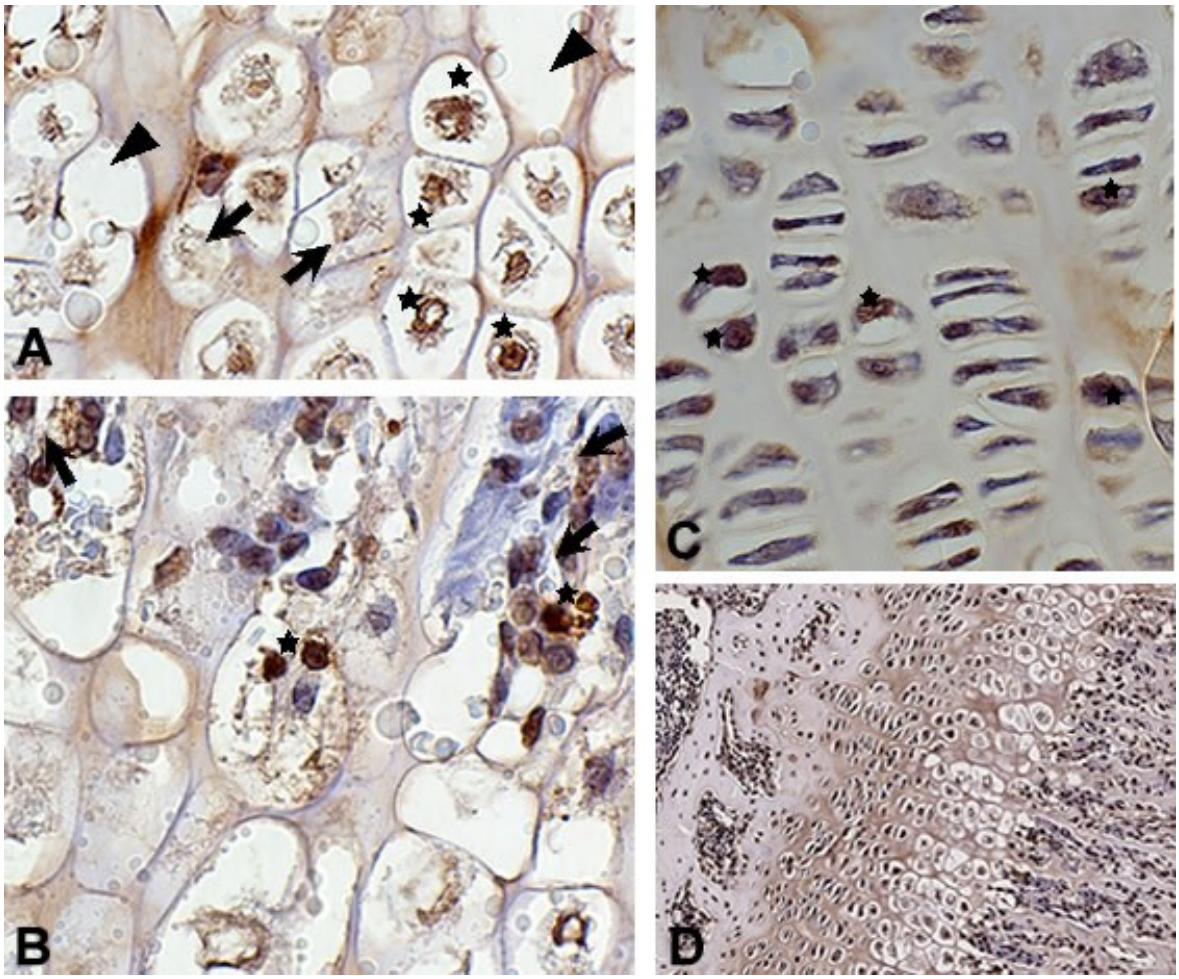

Figure 25: Light microscopy of several TUNEL-stained growth plate sections. *(A)* Hypertrophic chondrocytes. Note the empty lacunae (arrowheads), the lacunae with extracellular matrix and debris (arrows) and the TUNEL-positive chondrocytes (asterisks). *(B)* Lowermost hypertrophic zone, adjacent to the metaphysis. Ingrowth of vessels (arrows) accompanied by cells of mesenchymal origin, some of which are apoptotic (asterisks). Many lacunae which are devoid of a cell can be observed. *(C)* Proliferative chondrocytes arrange in columns. Apoptotic cells are marked with asterisks. *(D)* Tibial growth plate in its total length. The columnar zone can be easily distinguished from the hypertrophic zone. TUNEL method with hemalaun counterstain.

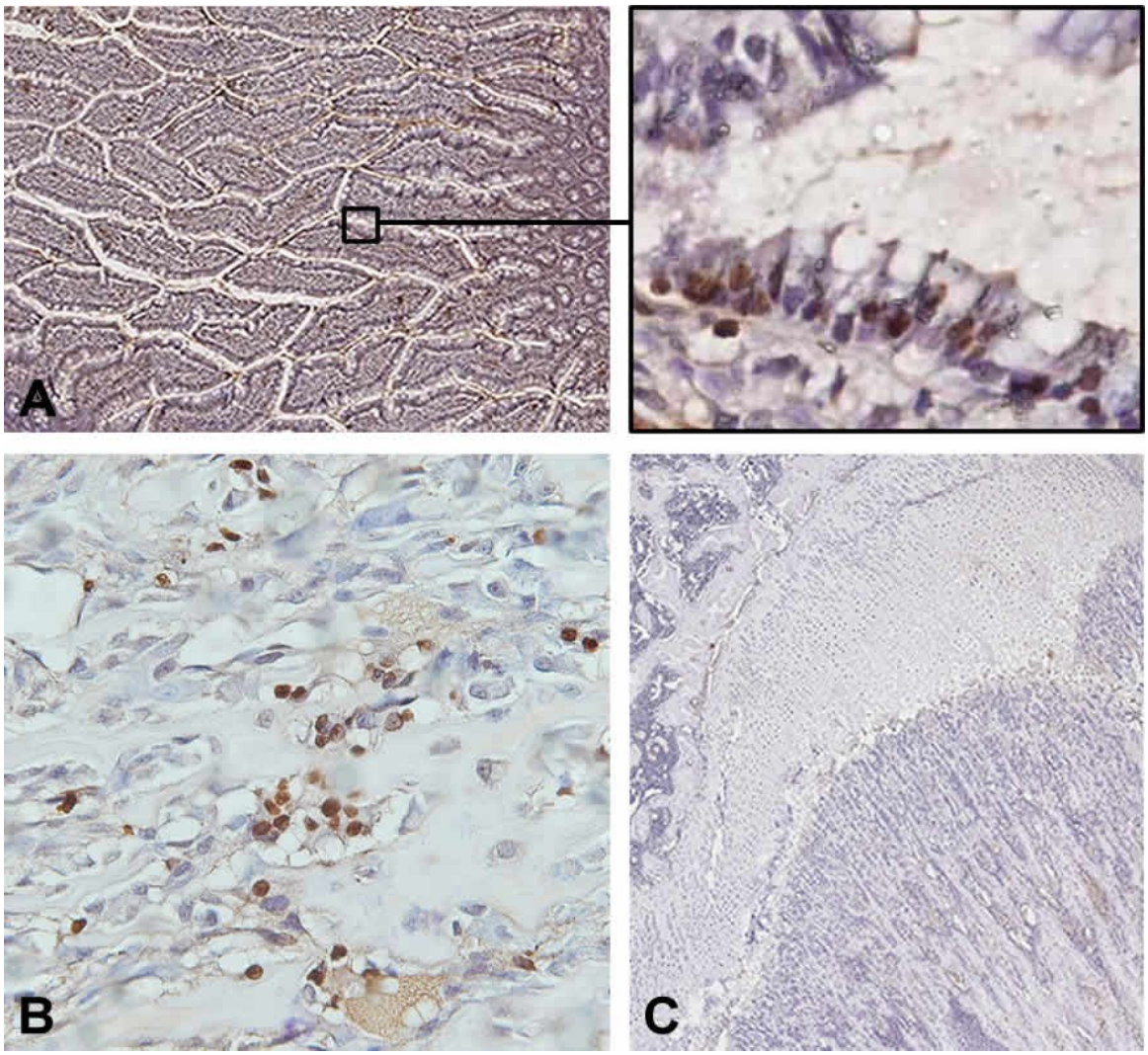

Figure 26: TUNEL method control sections. Positive controls were obtained on sections of rat small intestine *(A)*, additionally, bone marrow cells *(B)* served as an internal positive control. The brown colouring of cells indicates that they are apoptotic. Negative control specimens *(C)* did not show any TUNEL-positive cells since the enzyme TdT was omitted from reaction mixture. TUNEL method with hemalaun counterstain. Light microscopy.

5. DISCUSSION

Bone overgrowth is a clinically well known paediatric phenomenon which occurs after bone fracture, providing that the adjacent growth plate has not yet closed. Overgrowth after femoral fracture has been observed in a series of retrospective trials [7-11] and is to be obligatorily expected after any single fracture of growing long bones. Stimulating growth disturbances take place as a result of an enhanced stimulation of the nearby growth plates after fracture, which can affect the physis either wholly or partially, and may lead to limb length discrepancies and axial deformities, respectively. [4,5] However, up till now, the exact physeal response to fracture and the molecular mechanisms finally leading to growth disturbances have remained unclear and are the object of current research. Although the underlying molecular mechanisms which occur at the fracture site and which are responsible for the formation of callus and fracture healing have been elucidated to a certain extent [53-58], very little is known about the influence of fracture on the adjacent growth plate and its cellular and molecular events.

In order to gain better insight into post-fractural reactions and alterations of the growth plate after the occurrence of bone shaft fracture, the present study focused on the determination of physeal chondrocyte apoptosis in a rat model. It provides evidence that a middiaphyseal fracture in an animal model enhances chondrocyte apoptosis at the nearby growth plate.

5.1. The Rat Model

Much of the knowledge regarding the cellular and molecular biology of fracture healing has been enlightened by investigations conducted on rats. [53,55] Indeed, their bone development, with the formation of growth plates and primary and secondary ossification centres, resembles that of humans. The TUNEL-stained histological sections from this study revealed that the cellular architecture of the growth plate is almost identical to human growth plates.

Bonnarens and Einhorn developed a rat model for the production of a standard closed transverse experimental fracture by the use of a guillotine driven by a

dropped weight. Investigations on 40 male Sprague-Dawley rats confirmed that this closed fracture model meets the requirements of a reproducible, simple and inexpensive model. Fractures were highly reproducible in configuration and location and were accompanied by minimal soft tissue damage. They report uncomplicated fracture healing taking place in all rats. [80]

To summarise, the rat seems to serve as an ideal model for the study of bone fractures. However, the present study methods differ from clinical routine methods in the sense that in human patients fractures are stabilised by conservative or operative treatment, whereas the fractures of the experimental rats of this study were not immobilised. Hence, the remodelling capacity of growing bones could be utilised and maximum growth plate stimulation was achieved in order to demonstrate the stimulative effect of a fracture on the adjacent growth plate.

5.2. Fate of Hypertrophic Chondrocytes

Normal longitudinal growth during endochondral ossification depends on a well-defined process of maturational stages within the epiphyseal plate. [81] Chondrocytes of the human growth plate experience a life cycle which ranges from resting to proliferating before becoming hypertrophic cells and finally undergoing programmed cell death [45,46,82] with their apoptotic bodies supposedly phagocytosed by osteoclasts [83] (see also 2.2.3). Growth is achieved by chondrocyte proliferation, extracellular matrix deposition and mostly by chondrocyte hypertrophy. [46,81] Wilsman and collaborators discovered that in the proximal tibial growth plate, chondrocyte hypertrophy contributes to 60% of growth, cell proliferation to 10% of growth, and matrix deposition to the remainder. [84]

Up till now, there have been conflicting opinions on the ultimate fate of terminally differentiated hypertrophic chondrocytes. It is generally assumed that terminally differentiated hypertrophic cells must be deleted at the chondro-osseous junction in order to facilitate bone length growth and prevent continuing enlargement of the epiphyseal plate due to the constant cellular proliferation at the upper epiphyseal part of the physis. [81] However, there are several mechanisms of chondrocyte

deletion which have been proposed for over 100 years. [46] Some thought that hypertrophic chondrocytes would experience a dramatic change in shape, size, phenotype and gene expression and that they would convert to bone matrix-synthesising osteoblasts through a process of dedifferentiation and then redifferentiation, also referred to as transdifferentiation. [46,81] Definitive evidence of transdifferentiation is lacking. [81]

Today it is most widely accepted that terminally differentiated hypertrophic chondrocytes undergo programmed cell death by apoptosis [46]. Several studies confirmed the occurrence of chondrocyte apoptosis both in vitro [85,86] and in vivo [75,77,78] and some review articles refer to apoptosis as being the most likely mechanism of hypertrophic chondrocyte deletion [45,46,82].

However, further investigations support the incidence of variants of physiological cell death, which show ultrastructural morphological appearance that is different from the hallmark features of classical apoptosis. Roach and Clarke examined ultrastructural features of dying chondrocytes by means of electron microscopy and referred to examples of programmed cell death which do not involve apoptosis. They termed these cells “black chondrocytes” and “paralyzed cells” respectively, and described them to be “in limbo”, neither viable nor dead, and paralyzed in terms of function and not capable of damaging the surrounding area by inflammation. [87,88] Furthermore, Roach and Clarke assumed that this mode of non-apoptotic programmed cell death would occur in situations where phagocytosis of an apoptotic cell would not be possible such as in the case of chondrocyte confinement within the lacuna. [87,88] Later Roach and co-workers coined the term chondroptosis for the description of non-apoptotic physiological cell death found in chondrocytes. [89] In common with apoptotic cells, chondroptotic cells shrink and nuclear chromatin condenses. Unlike apoptosis, chondroptosis does not lead to the formation of apoptotic bodies but involves an initial increase of endoplasmic reticulum and Golgi apparatus, the formation of intracellular autophagic vacuoles used for self-degradation, and finally the extrusion of cellular remnants into the lacuna, resulting in the complete self-destruction of the chondrocyte and the appearance of an empty lacuna. Therefore, chondroptosis is not dependent on phagocytosis and may serve as an alternative

mechanism of cell deletion without inflammation for situations in which phagocytosis of apoptotic bodies would be difficult. [89] Shapiro and colleagues referred to a widespread death process termed autophagy or type II programmed cell death (apoptosis = type I programmed cell death) and preferred to use this term instead of chondroptosis. [81] Autophagy is not mediated by caspases but involves lysosomal proteinases, consequently the cell consumes itself. [81,89]

With regard to this study, which aims to determine the incidence of post-fractural physeal apoptosis by means of the TUNEL method, the disagreement about the ultimate fate of physeal hypertrophic chondrocytes (apoptosis versus chondroptosis/autophagy) influences the results in no way, since TUNEL is not capable of distinguishing apoptosis from chondroptosis and shows positive reactions in the occurrence of both mechanisms. [89] Moreover, the hypothesis of chondroptosis would feasibly explain the appearance of intact, empty and only debris-containing lacunae which could be constantly observed at the lowermost hypertrophic zone of the growth plate (Figure 25). In TUNEL-stained growth plate sections, Ploumis and collaborators also recognised a high number of terminal lacunae that were devoid of cells. He provided another possible reasoning for this discovery by suggesting that they would appear due to the loss of degenerating hypertrophic chondrocytes, discarded during staining processing. [75]

5.3. Apoptosis Detection with TUNEL – A Controversial Subject

Apoptosis can be detected by a variety of different techniques such as annexin V labelling, immunohistochemistry for caspases and apoptosis-related proteins, detection of DNA fragmentation by either the in situ nick end labelling method (TUNEL) or DNA agarose gel electrophoresis with the occurrence of a DNA ladder pattern, and the identification of characteristic ultrastructural morphologic changes under electron microscopy, which remains the most secure way to verify apoptotic death. In the present study TUNEL was used. It is a widely spread and easily applicable method [75], which is based on the specific TdT-catalysed binding of nucleotides to 3'-OH ends of nuclear DNA breaks [74]. Several previous studies have used this assay to identify apoptosis in chondrocytes. [75-78] Gavrieli and colleagues established this method as a specific, simple and reproducible tool for

the in situ detection of programmed cell death at a single-cell level whilst also preserving tissue architecture and enabling the additional visualisation of apoptotic morphological changes. [74]

Some researchers question the accuracy of TUNEL and postulate that false-negative and false-positive results lead to underestimation and overestimation, as well as to ambiguous and widely varying results. [89,90] For example, Chrysis and collaborators evaluated the apoptosis rate in rat growth plate and found that one quarter of the hypertrophic chondrocytes showed morphological characteristics of apoptosis although the number of TUNEL-positive cells was much lower. [77] Consequently, the data concerning the extent of apoptotic cells in the growth plate are quite controversial and vary widely, also due to the fact that investigations were carried out on different animal species at different ages. [75] Furthermore, growth rates and physeal activities differ depending on the origin of the epiphyseal plate. For instance, the human growth plates that are closer to the knee (distal femur, proximal tibia) show a higher level of activity than their opposite plates and contribute the most to longitudinal growth of the lower extremities. [46] Some studies estimate that the number of physeal apoptotic cells may be very low at a one-digit percentage level. [75,77,78] Another study found that up to a quarter of physeal cells would undergo apoptosis, dependent on the age of the animal. [91]

The present work revealed a high amount of physeal chondrocytes in apoptotic stages, reaching up to 25%, even in the control group. Although this result disagrees with several of the above mentioned studies, the conclusion that the fractured bone showed a significantly higher incidence of physeal apoptosis from day 3 onwards when compared to the contra-lateral bone, and from day 10 onwards when compared to the control bone, is still valid. The aim of this study was to compare the fractured, contra-lateral and control bone and not to determine the exact apoptosis rate in the growth plate. This apoptosis analysis should be seen more as a qualitative than a quantitative study. Therefore, the TUNEL apoptosis rate was not verified by additional methods, including immunohistochemistry for caspases and apoptosis-related proteins, DNA electrophoresis, or the evaluation of ultrastructural changes by the use of electron

microscopy, as some other authors demand [89,90] and have realised in their own apoptotic studies [75,77,78].

Furthermore, this study did not use additional staining of specific chondrocyte markers for the identification of this cell type or the biochemical distinction between proliferating and hypertrophic chondrocytes as TUNEL staining perfectly preserved the histology of the growth plate. Chondrocytes could thus be easily identified. Solely growth plate cells which formed columns were selected and assigned to the columnar proliferating zone. The resting zone of the epiphyseal plate was not evaluated. Enlarged cells surrounded by a lacuna were considered to be hypertrophic cells. Cells in the so-called transition zone that could not be definitely classified as columnar or hypertrophic cells were not counted. In the lowermost hypertrophic zone with vascular ingrowth it was not always clear whether an apoptotic cell in an open lacuna belonged to the hypertrophic cells or was of mesenchymal origin. In such cases of uncertainty, the cell was skipped and not evaluated.

The manual counting of the cells turned out to be extremely time-consuming. It also involves the risk of a bias. An automated counting by means of appropriate software was not possible, since the colour as well as morphological changes had to be considered and the intensity of counterstaining varied in each staining run.

5.4. Increased Growth Plate Apoptosis after Fracture

This study reveals that the number of chondrocyte programmed cell deaths is significantly higher in the growth plate of fractured bones compared to both the contra-lateral intact bone and the control bone. Furthermore, the lack of a significant increase of apoptotic cells in the intact contra-lateral bone when compared to the control-bone suggests that the fracture influences chondrocyte apoptosis of the adjacent growth plate via a local effect. A systemic effect of the fracture would have additionally influenced the contra-lateral epiphyseal plate.

The death and removal of terminally differentiated hypertrophic chondrocytes provides space for the ingrowth of new blood vessels that bring bone cell

precursors, osteoblasts, osteoclasts and chondroclasts. [45-47,82] Programmed cell death of hypertrophic chondrocytes is thus associated with cartilage resorption and bone replacement, which are essential for longitudinal bone growth.

5.5. Age-dependency of Physeal Chondrocyte Apoptosis

This work affirms the assumption that the extent of chondrocyte apoptosis during normal development depends on the age of the species [75,77,91]. Aizawa and co-workers found out that the number of TUNEL-positive cells in growth plates of rabbits increases with growth and age, while the number of proliferating chondrocytes decreases. [91] Regarding control animals, this study shows a statistically significant increase of chondrocyte apoptosis from day 14 to 29, whereas the apoptosis rate of the fractured bones tends to rise over time without statistical significance.

5.6. Columnar versus Hypertrophic Chondrocytes

Another finding of the present work was the constantly higher number of TUNEL-positive cells in the proliferating zone than in the hypertrophic zone. Some studies have already demonstrated TUNEL-positive cells in the hypertrophic zone and also in the resting and proliferating zones [75,77,91], but with the highest rate of apoptosis in the hypertrophic zone. Given that empty lacunae and lacunae containing only debris or extracellular matrix were not counted as apoptotic cell bodies in our study, the higher incidence of apoptosis in the columnar zone could be partly caused by this kind of cell counting. Moreover, some apoptotic hypertrophic cells could have been discarded during the staining process. The conclusion that the rate of physeal cellular deletion must be the same as the rate at which the cells proliferate [81], combined with the assumption that bone fracture would stimulate the proliferation of growth plate chondrocytes, serves as a comprehensible explanation for the higher apoptosis rate, even among proliferative chondrocytes. Ploumis and colleagues also assumed that the DNA fragmentation would start early in the process of chondrocyte differentiation. [75]

This innovative work successfully demonstrated that bone fracture during growth affects the growth plate. In conclusion, the physeal apoptosis rate of the fractured bone was significantly higher in comparison to the contra-lateral intact bone (valid for all evaluated days) and to the control bone (valid from day 10 onwards). The lack of a significant difference between the intact contra-lateral and the intact control bone suggests that the local effect on the adjacent physis overlaps the systemic effect which would additionally influence the contra-lateral epiphyseal plate.

The type of local effect which leads to post-traumatic elevated programmed cell death remains unclear. The influence of certain cytokines and hormones such as TNF-α and FGFs, the down regulation of PTHrP – a known potent inhibitor of chondrocyte apoptosis [45] – or a higher chondrocyte proliferation rate may be considered as possible stimuli for a programmed cell death, occurring more often in physeal chondrocytes after fracture. The latter supports the idea that an increased number of hypertrophic chondrocytes would lead to the release of more matrix vesicles containing alkaline phosphatase, an enzyme that increases the concentration of phosphate ions, necessary for the calcification process. Phosphate is suggested to trigger apoptosis by promoting mitochondrial membrane permeability transition, leading to mitochondrial release of cytochrome c. [45]

Nevertheless, the above mentioned explanations for the exact stimulus leading to the increased apoptosis rate after fracture remain hypotheses which would require additional research to be supported.

REFERENCES

1. Breitfuss H, Weinberg A-M, Muhr G. Wachstumsphänomene bei Frakturen im Kindesalter: Spontankorrekturen und Wachstumsstörungen. In: Weinberg A-M, Tscherne H, editors. Tscherne Unfallchirurgie: Unfallchirurgie im Kindesalter. Berlin Heidelberg New York: Springer; 2006. p. 39-49.

2. von Laer L, Hasler C. [Spontaneous corrections, growth disorders and post-traumatic deformities after fractures in the area of the forearm of the growing skeleton]. Handchir Mikrochir Plast Chir 2000 Jul;32(4):231-41.

3. von Laer L, Kraus R. [Conservative treatment of fractures of the long bones during the growth phase]. Unfallchirurg 2007 Oct;110(10):811-23.

4. Linhart WE, von Laer L. [General considerations in the management of paediatric injuries]. Orthopade 2005 Nov;34(11):1169-84.

5. Hasler CC, von Laer L. [Pathophysiology of posttraumatic deformities of the lower limbs during growth]. Orthopade 2000 Sep;29(9):757-65.

6. Hasler CC. [Leg length inequality. Indications for treatment and importance of shortening procedures]. Orthopade 2000 Sep;29(9):766-74.

7. Clement DA, Colton CL. Overgrowth of the femur after fracture in childhood. An increased effect in boys. J Bone Joint Surg Br 1986 Aug;68(4):534-6.

8. Edvardsen P, Syversen SM. Overgrowth of the femur after fracture of the shaft in childhood. J Bone Joint Surg Br 1976 Aug;58(3):339-42.

9. Reynolds DA. Growth changes in fractured long-bones: a study of 126 children. J Bone Joint Surg Br 1981 Feb;63-B(1):83-8.

10. Stephens MM, Hsu LC, Leong JC. Leg length discrepancy after femoral shaft fractures in children. Review after skeletal maturity. J Bone Joint Surg Br 1989 Aug;71(4):615-8.

11. Zimmermann R, Stoger A, Golser K, Gabl M, Angermann P, Benedetto K. [Tibial growth after isolated femoral shaft fracture in the growth stage]. Unfallchirurg 1999 May;102(5):365-70.

12. von Laer L, Kaelin L, Girard T. [Late results following shaft fractures of the lower extremities in the growth period]. Z Unfallchir Versicherungsmed Berufskr 1989;82(4):209-15.

13. Laer Lv, Herzog B. [Leg length differences and rotation defects after femoral shaft fractures in childhood. Therapeutic influence and spontaneous correction]. Helv Chir Acta 1978 May;45(1-2):17-21.

14. Meyer U, Wiesmann HP. Bone and cartilage engineering. Berlin Heidelberg New York: Springer-Verlag; 2006.

15. Pocock G, Richards CD. Human physiology: the basis of medicine. 3rd ed. New York: Oxford University Press; 2006. p. 498-503.

16. Ganong WF. Review of medical physiology. 22nd ed. New York: The McGraw-Hill Companies; 2005. p. 382-95.

17. Cohen MM, Jr. The new bone biology: pathologic, molecular, and clinical correlates. Am J Med Genet A 2006 Dec 1;140(23):2646-706.

18. Boron WF, Boulpaep EL. Medical physiology: a cellular and molecular approach. Philadelphia: Elsevier Saunders; 2005. p. 1088-91.

19. Standring S, Ellis H, Healy JC, Johnson D, Williams A, Collins P, et al. Gray's anatomy: the anatomical basis of clinical practice. 29th ed. Edinburgh: Elsevier Churchill Livingstone; 2005. p. 83-104.

20. Schuenke M, Schulte E, Schumacher U. Atlas of anatomy. Stuttgart: Georg Thieme Verlag; 2006.

21. Weinberg A-M, Hofmann A, Claus P. Molekulare, physiologische und anatomische Grundlagen der Knochenentwicklung. In: Weinberg A-M, Tscherne H, editors. Tscherne Unfallchirurgie: Unfallchirurgie im Kindesalter. Berlin Heidelberg New York: Springer; 2006. p. 3-14.

22. Faller A, Schuenke M, Schuenke G. The human body: an introduction to structure and function. Stuttgart: Georg Thieme Verlag; 2004. p. 116-7.

23. Allen MR, Hock JM, Burr DB. Periosteum: biology, regulation, and response to osteoporosis therapies. Bone 2004 Nov;35(5):1003-12.

24. Kuehnel W. Color atlas of cytology, histology, and microscopic anatomy. 4th ed. Stuttgart: Georg Thieme Verlag; 2003. p. 154-7.

25. Bucher O, Wartenberg H. Cytologie, Histologie und mikroskopische Anatomie des Menschen. 12th ed. Bern: Verlag Hans Huber; 1997. p. 101-41.

26. Noble BS, Reeve J. Osteocyte function, osteocyte death and bone fracture resistance. Mol Cell Endocrinol 2000 Jan 25;159(1-2):7-13.

27. Robey PG. Vertebrate mineralized matrix proteins: structure and function. Connect Tissue Res 1996;35(1-4):131-6.

28. Katagiri T, Takahashi N. Regulatory mechanisms of osteoblast and osteoclast differentiation. Oral Dis 2002 May;8(3):147-59.

29. Aubin JE, Liu F, Malaval L, Gupta AK. Osteoblast and chondroblast differentiation. Bone 1995 Aug;17(2 Suppl):77S-83S.

30. Aubin JE, Turksen K. Monoclonal antibodies as tools for studying the osteoblast lineage. Microsc Res Tech 1996 Feb 1;33(2):128-40.

31. Kessler E, Takahara K, Biniaminov L, Brusel M, Greenspan DS. Bone morphogenetic protein-1: the type I procollagen C-proteinase. Science 1996 Jan 19;271(5247):360-2.

32. Granjeiro JM, Oliveira RC, Bustos-Valenzuela JC, Sogayar MC, Taga R. Bone morphogenetic proteins: from structure to clinical use. Braz J Med Biol Res 2005 Oct;38(10):1463-73.

33. Kobayashi T, Kronenberg H. Minireview: transcriptional regulation in development of bone. Endocrinology 2005 Mar;146(3):1012-7.

34. Dobnig H, Turner RT. Evidence that intermittent treatment with parathyroid hormone increases bone formation in adult rats by activation of bone lining cells. Endocrinology 1995 Aug;136(8):3632-8.

35. Pead MJ, Skerry TM, Lanyon LE. Direct transformation from quiescence to bone formation in the adult periosteum following a single brief period of bone loading. J Bone Miner Res 1988 Dec;3(6):647-56.

36. Gerstenfeld LC. Osteopontin in skeletal tissue homeostasis: An emerging picture of the autocrine/paracrine functions of the extracellular matrix.[comment]. J Bone Miner Res 1999 Jun;14(6):850-5.

37. Udagawa N, Takahashi N, Akatsu T, Tanaka H, Sasaki T, Nishihara T, et al. Origin of osteoclasts: mature monocytes and macrophages are capable of differentiating into osteoclasts under a suitable microenvironment prepared by bone marrow-derived stromal cells. Proc Natl Acad Sci U S A 1990 Sep;87(18):7260-4.

38. Roodman GD. Advances in bone biology: the osteoclast. Endocr Rev 1996 Aug;17(4):308-32.

39. Teitelbaum SL. Osteoclasts and integrins. Ann N Y Acad Sci 2006 Apr;1068:95-9.

40. Teitelbaum SL. Osteoclasts: what do they do and how do they do it? Am J Pathol 2007 Feb;170(2):427-35.

41. Yuasa K, Mori K, Ishikawa H, Sudo A, Uchida A, Ito Y. Characterization of two types of osteoclasts from human peripheral blood monocytes. Biochem Biophys Res Commun 2007 May 4;356(2):354-60.

42. Udagawa N, Takahashi N, Jimi E, Matsuzaki K, Tsurukai T, Itoh K, et al. Osteoblasts/stromal cells stimulate osteoclast activation through expression of osteoclast differentiation factor/RANKL but not macrophage colony-stimulating factor: receptor activator of NF-kappa B ligand. Bone 1999 Nov;25(5):517-23.

43. Rivas R, Shapiro F. Structural stages in the development of the long bones and epiphyses: a study in the New Zealand white rabbit. J Bone Joint Surg Am 2002 Jan;84-A(1):85-100.

44. Kronenberg HM. Developmental regulation of the growth plate. Nature 2003 May 15;423(6937):332-6.

45. Ballock RT, O'Keefe RJ. The biology of the growth plate. J Bone Joint Surg Am 2003 Apr;85-A(4):715-26.

46. Forriol F, Shapiro F. Bone development: interaction of molecular components and biophysical forces. Clin Orthop 2005 Mar;432:14-33.

47. Rauch F. Bone growth in length and width: the Yin and Yang of bone stability. J 2005 Jul-Sep;5(3):194-201.

48. Abad V, Meyers JL, Weise M, Gafni RI, Barnes KM, Nilsson O, et al. The role of the resting zone in growth plate chondrogenesis. Endocrinology 2002 May;143(5):1851-7.

49. Seeman E. Periosteal bone formation - a neglected determinant of bone strength.[comment]. N Engl J Med 2003 Jul 24;349(4):320-3.

50. Mehlman CT, Araghi A, Roy DR. Hyphenated history: the Hueter-Volkmann law. Am J Orthop 1997 Nov;26(11):798-800.

51. Provot S, Schipani E. Molecular mechanisms of endochondral bone development. Biochem Biophys Res Commun 2005 Mar 18;328(3):658-65.

52. Ehlen HWA, Buelens LA, Vortkamp A. Hedgehog signaling in skeletal development. Birth Defects Res Part C Embryo Today 2006 Sep;78(3):267-79.

53. Einhorn TA. The cell and molecular biology of fracture healing. Clin Orthop 1998 Oct(355 Suppl):S7-21.

54. Gerstenfeld LC, Einhorn TA. Developmental aspects of fracture healing and the use of pharmacological agents to alter healing. J 2003 Dec;3(4):297-303.

55. Tsiridis E, Upadhyay N, Giannoudis P. Molecular aspects of fracture healing: which are the important molecules? Injury 2007 Mar;38:11-25.

56. Einhorn TA. The science of fracture healing. J Orthop Trauma 2005 Nov-Dec;19(10 Suppl):S4-6.

57. Landry PS, Marino AA, Sadasivan KK, Albright JA. Bone injury response. An animal model for testing theories of regulation. Clin Orthop 1996 Nov;332:260-73.

58. Gerstenfeld LC, Cullinane DM, Barnes GL, Graves DT, Einhorn TA. Fracture healing as a post-natal developmental process: molecular, spatial, and temporal aspects of its regulation. J Cell Biochem 2003 Apr 1;88(5):873-84.

59. Lee FY, Choi YW, Behrens FF, DeFouw DO, Einhorn TA. Programmed removal of chondrocytes during endochondral fracture healing. J Orthop Res 1998 Jan;16(1):144-50.

60. Einhorn TA, Majeska RJ, Rush EB, Levine PM, Horowitz MC. The expression of cytokine activity by fracture callus. J Bone Miner Res 1995 Aug;10(8):1272-81.

61. Kon T, Cho TJ, Aizawa T, Yamazaki M, Nooh N, Graves D, et al. Expression of osteoprotegerin, receptor activator of NF-kappaB ligand (osteoprotegerin ligand) and related proinflammatory cytokines during fracture healing. J Bone Miner Res 2001 Jun;16(6):1004-14.

62. Gerstenfeld LC, Cho TJ, Kon T, Aizawa T, Tsay A, Fitch J, et al. Impaired fracture healing in the absence of TNF-alpha signaling: the role of TNF-alpha in endochondral cartilage resorption. J Bone Miner Res 2003 Sep;18(9):1584-92.

63. Cho T-J, Gerstenfeld LC, Einhorn TA. Differential temporal expression of members of the transforming growth factor beta superfamily during murine fracture healing. J Bone Miner Res 2002 Mar;17(3):513-20.

64. Jones PF. Not just angiogenesis - wider roles for the angiopoietins. J Pathol 2003 Dec;201(4):515-27.

65. Baynes JW, Dominiczak MH. Medical biochemistry. 2nd ed. Philadelphia: Elsevier Mosby; 2005. p. 590-3.

66. Jacobson MD, Weil M, Raff MC. Programmed cell death in animal development. Cell 1997 Feb 7;88(3):347-54.

67. Lodish H, Berk A, Kaiser CA, Krieger M, Scott MP, Bretscher A, et al. Molecular cell biology. 6th ed. New York: W. H. Freeman and Company; 2008. p. 936-44.

68. Lemasters JJ. Dying a thousand deaths: redundant pathways from different organelles to apoptosis and necrosis. Gastroenterology 2005 Jul;129(1):351-60.

69. van Engeland M, Nieland LJ, Ramaekers FC, Schutte B, Reutelingsperger CP. Annexin V-affinity assay: a review on an apoptosis detection system based on phosphatidylserine exposure. Cytometry 1998 Jan 1;31(1):1-9.

70. Nieminen AI, Partanen JI, Klefstrom J. c-Myc blazing a trail of death: coupling of the mitochondrial and death receptor apoptosis pathways by c-Myc. Cell Cycle 2007 Oct 15;6(20):2464-72.

71. Rangamani P, Sirovich L. Survival and apoptotic pathways initiated by TNF-alpha: modeling and predictions. Biotechnol Bioeng 2007 Aug 1;97(5):1216-29.

72. Hollier M, Whistler T, Dawson C, Vernon SD. Two optimized combination assays to examine apoptosis pathways in clinical samples. Cytometry A 2007 Sep;71(9):675-85.

73. Roche Diagnostics Corporations. Apoptosis, cell death, and cell proliferation manual. 2004/2005 [cited 2007 Dec 20]. Available from: URL:www.roche-applied-science.com/PROD_INF/MANUALS/CELL_MAN/cell_toc.html

74. Gavrieli Y, Sherman Y, Ben-Sasson SA. Identification of programmed cell death in situ via specific labeling of nuclear DNA fragmentation. J Cell Biol 1992 Nov;119(3):493-501.

75. Ploumis A, Manthou M-E, Emmanouil-Nikolousi E-N, Androudi S, Christodoulou A. Animal model of chondrocyte apoptosis in the epiphyseal cartilage of the neonatal bone. J Orthop Sci 2004;9(5):495-502.

76. Silvestrini G, Mocetti P, Ballanti P, Di Grezia R, Bonucci E. In vivo incidence of apoptosis evaluated with the TdT FragEL DNA fragmentation detection kit in cartilage and bone cells of the rat tibia. Tissue & Cell 1998 Dec;30(6):627-33.

77. Chrysis D, Nilsson O, Ritzen EM, Savendahl L. Apoptosis is developmentally regulated in rat growth plate. Endocrine 2002 Aug;18(3):271-8.

78. Zenmyo M, Komiya S, Kawabata R, Sasaguri Y, Inoue A, Morimatsu M. Morphological and biochemical evidence for apoptosis in the terminal hypertrophic chondrocytes of the growth plate. J Pathol 1996 Dec;180(4):430-3.

79. Nagata S, Nagase H, Kawane K, Mukae N, Fukuyama H. Degradation of chromosomal DNA during apoptosis. Cell Death Differ 2003 Jan;10(1):108-16.

80. Bonnarens F, Einhorn TA. Production of a standard closed fracture in laboratory animal bone. J Orthop Res 1984;2(1):97-101.

81. Shapiro IM, Adams CS, Freeman T, Srinivas V. Fate of the hypertrophic chondrocyte: microenvironmental perspectives on apoptosis and survival in the epiphyseal growth plate. Birth Defects Res Part C Embryo Today 2005 Dec;75(4):330-9.

82. Shum L, Nuckolls G. The life cycle of chondrocytes in the developing skeleton. Arthritis Res 2002;4(2):94-106.

83. Bronckers AL, Goei W, van Heerde WL, Dumont EA, Reutelingsperger CP, van den Eijnde SM. Phagocytosis of dying chondrocytes by osteoclasts in the mouse growth plate as demonstrated by annexin-V labelling. Cell Tissue Res 2000 Aug;301(2):267-72.

84. Wilsman NJ, Farnum CE, Leiferman EM, Fry M, Barreto C. Differential growth by growth plates as a function of multiple parameters of chondrocytic kinetics. J Orthop Res 1996 Nov;14(6):927-36.

85. Cheung JOP, Grant ME, Jones CJP, Hoyland JA, Freemont AJ, Hillarby MC. Apoptosis of terminal hypertrophic chondrocytes in an in vitro model of endochondral ossification. J Pathol 2003 Nov;201(3):496-503.

86. Gibson G, Lin DL, Roque M. Apoptosis of terminally differentiated chondrocytes in culture. Exp Cell Res 1997 Jun 15;233(2):372-82.

87. Roach HI, Clarke NM. "Cell paralysis" as an intermediate stage in the programmed cell death of epiphyseal chondrocytes during development. J Bone Miner Res 1999 Aug;14(8):1367-78.

88. Roach HI, Clarke NM. Physiological cell death of chondrocytes in vivo is not confined to apoptosis. New observations on the mammalian growth plate. J Bone Joint Surg Br 2000 May;82(4):601-13.

89. Roach HI, Aigner T, Kouri JB. Chondroptosis: a variant of apoptotic cell death in chondrocytes? Apoptosis 2004 May;9(3):265-77.

90. Aigner T. Chondrocyte apoptosis in osteoarthritis: comment on the letter by Kouri and Abbud-Lozoya. Arthritis Rheum 2003 Apr;48(4):1166-7.

91. Aizawa T, Kokubun S, Tanaka Y. Apoptosis and proliferation of growth plate chondrocytes in rabbits. J Bone Joint Surg Br 1997 May;79(3):483-6.